Title

Promotion of Cell Viability and Histone Gene Expression by the Acetyltransferase Gcn5 and the Protein Phosphatase PP2A in Saccharomyces cerevisiae

Journal

Genetics, 203(4)

ISSN

0016-6731

Authors

Petty, Emily L
Lafon, Anne
Tomlinson, Shannon L
et al.

Publication Date

2016-08-01

DOI

10.1534/genetics.116.189506

Peer reviewed

Promotion of Cell Viability and Histone Gene Expression by the Acetyltransferase Gcn5 and the Protein Phosphatase PP2A in *Saccharomyces cerevisiae*

Emily L. Petty, Anne Lafon,[1] Shannon L. Tomlinson, Bryce A. Mendelsohn,[2] and Lorraine Pillus[3]
Division of Biological Sciences, Molecular Biology, University of California, San Diego Moores Cancer Center, La Jolla, California 92093
ORCID IDs: 0000-0001-5932-9044 (E.L.P.); 0000-0002-8818-5227 (L.P.)

ABSTRACT Histone modifications direct chromatin-templated events in the genome and regulate access to DNA sequence information. There are multiple types of modifications, and a common feature is their dynamic nature. An essential step for understanding their regulation, therefore, lies in characterizing the enzymes responsible for adding and removing histone modifications. Starting with a dosage-suppressor screen in *Saccharomyces cerevisiae*, we have discovered a functional interaction between the acetyltransferase Gcn5 and the protein phosphatase 2A (PP2A) complex, two factors that regulate post-translational modifications. We find that *RTS1*, one of two genes encoding PP2A regulatory subunits, is a robust and specific high-copy suppressor of temperature sensitivity of *gcn5*Δ and a subset of other *gcn5*Δ phenotypes. Conversely, loss of both PP2A^{Rts1} and Gcn5 function in the SAGA and SLIK/SALSA complexes is lethal. *RTS1* does not restore global transcriptional defects in *gcn5*Δ; however, histone gene expression is restored, suggesting that the mechanism of *RTS1* rescue includes restoration of specific cell cycle transcripts. Pointing to new mechanisms of acetylation–phosphorylation cross-talk, *RTS1* high-copy rescue of *gcn5*Δ growth requires two residues of H2B that are phosphorylated in human cells. These data highlight the potential significance of dynamic phosphorylation and dephosphorylation of these deeply conserved histone residues for cell viability.

KEYWORDS chromatin; transcription; phosphorylation; acetylation (*IOC2*, *PAB1*, *RHO2*, *MED6*, *ZDS1*, PP2A^{B56})

At the foundation of nuclear DNA organization in eukaryotes is the dynamic formation, movement, and modification of nucleosomes. Acetylation and phosphorylation are two histone post-translational modifications (PTMs) catalyzed by histone acetyltransferases (HATs) and kinases and reversed by histone deacetylases (HDACs) and phosphatases that alter nucleosome structure and function. Tightly regulated acetylation and phosphorylation of specific histone residues have deeply conserved functions in eukaryotes that are critical for transcriptional regulation, replication, repair, and segregation of eukaryotic genomes (Banerjee and Chakravarti 2011; Rossetto *et al.* 2012; Tessarz and Kouzarides 2014).

One well-conserved HAT is Gcn5, which specifically targets histones H3 and H2B as part of multiple complexes (Grant *et al.* 1997; Eberharter *et al.* 1999; Grant *et al.* 1999; Howe *et al.* 2001; Sterner *et al.* 2002; Pray-Grant *et al.* 2005). Gcn5 is a key regulator of eukaryotic gene expression and acetylates H3 at promoters of active genes (Pokholok *et al.* 2005; Nagy and Tora 2007; Rosaleny *et al.* 2007). Its role as a transcriptional activator is so fundamental that Gcn5 is essential in most eukaryotes studied. An exception of note is budding yeast, where deletion of *GCN5* is tolerated, but does cause a spectrum of phenotypes, including defects in gene activation, particularly for stress-regulated genes, and altered cell cycle progression (Howe *et al.* 2001; Huisinga and Pugh 2004; Vernarecci *et al.* 2008). Gcn5-mediated histone acetylation does not function in isolation, but is affected by other PTMs. For example, H3S10 phosphorylation

doi: 10.1534/genetics.116.189506
Manuscript received March 21, 2016; accepted for publication May 27, 2016; published Early Online June 14, 2016.
Supplemental material is available online at www.genetics.org/lookup/suppl/doi:10.1534/genetics.116.189506/-/DC1.
[1]Present address: Institut Curie, Unité mixte de recherche 3664 Centre national de la recherche scientifique, 75248 Paris Cedex 05, France.
[2]Present address: Department of Pediatrics, Division of Medical Genetics, University of California, San Francisco, 550 16th Street #0706, San Francisco, CA 94158.
[3]Corresponding author: University of California, San Diego, 9500 Gilman Dr., La Jolla, CA 92093-0347. E-mail: lpillus@ucsd.edu

(H3S10ph) promotes H3-K14 acetylation (H3K14ac) in mammals and yeast (Cheung *et al.* 2000; Lo *et al.* 2000). The full extent to which acetylation by Gcn5 interacts with other dynamic modifications remains an active area of investigation.

Nuclear functions of Gcn5 in eukaryotes extend beyond transcriptional regulation into response to DNA damage and nucleosome reassembly during genome replication. Acetylation of H3K9 by Gcn5 promotes nucleotide excision repair in human cells (Guo *et al.* 2011) and recruits the chromatin remodeling complex SWI/SNF to sites of double-stranded breaks in yeast and human cells to promote repair (Lee *et al.* 2010; Bennett and Peterson 2015). During genome replication, H3 acetylation by Gcn5 recruits histone chaperones leading to assembly of new nucleosomes (Burgess *et al.* 2010). Therefore, Gcn5 has integral roles in genome maintenance and organization.

Among enzymes controlling dynamic phosphorylation, PP2A is a conserved heterotrimeric serine/threonine phosphatase complex consisting of catalytic (encoded by *PPH21* and *PPH22*), regulatory (encoded by *CDC55* and *RTS1*), and structural (encoded by *TPD3*) subunits in yeast (Jiang 2006). Humans have 15 regulatory subunits (also known as B subunits), resulting in formation of dozens of biochemically distinct forms of PP2A (Virshup and Shenolikar 2009). Cdc55 and Rts1 are homologous to the mammalian B55 and B56 subunits, respectively. Human forms of PP2A complexes have been implicated in multiple cancers with specific B56 isoforms functioning as tumor suppressors (Yang and Phiel 2010; Seshacharyulu *et al.* 2013). Impaired $PP2A^{B56}$ function is also associated with neurological disorders such as Alzheimer's disease (Sontag and Sontag 2014).

The relative simplicity of PP2A as $PP2A^{Cdc55}$ and $PP2A^{Rts1}$ forms has made yeast an ideal organism in which to characterize distinct functions of PP2A. Indeed, several previous studies have found nonoverlapping roles for the two PP2A complexes in many aspects of cell function, particularly in regulating chromatin dynamics during the cell cycle. $PP2A^{Cdc55}$ contributes to progression through the G2/M checkpoint and prevents early mitotic exit (Queralt *et al.* 2006; Wang and Ng 2006; Yellman and Burke 2006; Rossio and Yoshida 2011). $PP2A^{Rts1}$ localizes to centromeric chromatin, where it promotes condensin loading and functions in the tension-sensing mechanism of the spindle assembly checkpoint (Chan and Amon 2009; Nerusheva *et al.* 2014; Peplowska *et al.* 2014; Verzijlbergen *et al.* 2014). Further, $PP2A^{Rts1}$ coordinately regulates cell cycle entry and the cell size checkpoint, in part by relieving transcriptional repression of the G1 cyclin Cln3, but the mechanism of this control is not yet fully defined (Artiles *et al.* 2009; Zapata *et al.* 2014).

We report here a functional interaction between the Gcn5 acetyltransferase and $PP2A^{Rts1}$ phosphatase that is critical for cell viability and cell cycle progression. We found that overexpression of *RTS1* rescues multiple *gcn5*Δ mutant phenotypes, including temperature sensitivity, DNA damage sensitivity, and progression though S phase. Deepening this acetyl–phospho connection, we found that concurrent loss of SAGA and/or SLIK/SALSA and $PP2A^{Rts1}$ function is lethal. This demonstrates that the coordinated functions of these enzymatic complexes are critical for cell viability. We determined that *gcn5*Δ cells have reduced histone protein and messenger RNA (mRNA) levels, both of which are rescued by *RTS1* overexpression. Lastly, in a directed "histome"-wide screen of core histone residues potentially subject to phosphorylation, we identified two conserved residues of H2B that are required for rescue of *gcn5*Δ by *RTS1* overexpression.

Materials and Methods

Yeast growth, strains, and plasmids

All strains used in this study are in the W303 background and listed in Supplemental Material, Table S1. Standard conditions were used to grow and maintain strains on YPAD (yeast extract-peptone-dextrose + adenine) or synthetic dropout liquid and solid medium (Guthrie and Fink 1991). For selection against *URA3* plasmids, 5-FOA was used at 0.1%. All other drug additives or media substitutions are specified in the figure legends. Liquid minimal sporulation medium was used for diploids prior to tetrad dissection and genotyping (Rose *et al.* 1990). Transformants and deletion mutants were constructed with standard methods (Amberg *et al.* 2005) using plasmids listed in Table S2 and oligonucleotides in Table S3. A 2μ-plasmid library (Engebrecht *et al.* 1990) was used for the suppressor screen of *gcn5*Δ *sas3-C357Y, P375A* (Howe *et al.* 2001) temperature sensitivity. Briefly, the library was transformed into LPY13321 (*gcn5*Δ::*natMX sas3*Δ::*HIS3 ura3-1*::*sas3 C357Y, P375A-URA3*). Transformants were plated on YPAD to recover for 36 hr before replica plating onto Leu^- containing 1 M sorbitol and grown at 37° to select suppressors. Sorbitol was used to increase screen sensitivity. Sequencing with universal oligonucleotides flanking each library insert identified endpoints of the chromosomal fragments in the rescuing plasmids. Subcloning individual genes within the insert was used to identify the suppressing gene. The phosphohistome screen was performed with the SHIMA histone mutant library, (Nakanishi *et al.* 2008). Site-directed mutagenesis was used to generate other mutants. For plate assays, overnight cultures were diluted to 1 O.D. A_{600} and 1:5 serial dilutions were plated and imaged after 3–5 days. Images of plate assays are representative of at least three biological replicates with freshly transformed strains.

α-Factor arrest and flow cytometry

LPY11975 (*bar1*Δ::*kanMX*) and LPY21272 (*gcn5*Δ::*natMX bar1*Δ::*kanMX*) were transformed with pLP136 (2μ vector) or pLP2462 (2μ *RTS1*) and cultures of fresh transformants were grown in Ura^- overnight. Cultures were diluted to 0.1 O.D. A_{600} in YPAD, grown to 0.2–0.3 O.D. A_{600}, and arrested with α-factor (200 μg/ml for LPY11975 and 40 μg/ml for LPY 21272) for 90–120 min at 30°. Cells were washed twice with fresh, prewarmed YPAD to release and grow at 30° or 37°.

Samples were collected immediately and 30 min after release for analysis (Haase and Reed 2002) using a BD Accuri C6 Flow Cytometer. The *bar1*Δ mutation facilitated synchronization by enhancing pheromone sensitivity (Amberg *et al.* 2006).

Okadaic acid survival assay

Overnight cultures of LPY5 [wild type (WT)] and LPY10182 (*gcn5*Δ::*kanMX*) transformed with either vector (pLP136) or *RTS1* (pLP2462) 2μ plasmids were diluted to 0.1 O.D. A_{600} and grown to 0.4 O.D. A_{600} at 30°. A total of 10 μM of okadaic acid (OKA) sodium salt (LC Labs, O-5857) or an equal volume of DMSO (solvent) was added to the cultures and cells were grown for 1 hr as in Peplowska *et al.* (2014). Cells were then spread onto prewarmed plates at 500–1000 cells per plate. Colonies were counted after 3 days for 30° plates, and 4 days for 36.5° plates. The ratio of 36.5°:30° CFU was calculated to determine high-temperature survival after OKA and ratios were normalized to WT + vector. Three independent experiments were conducted, each with independently transformed strains.

Protein lysates and immunoblotting

Whole cell extracts were prepared as described (Clarke *et al.* 1999). For preservation of phosphorylated species, OKA (2 nM), sodium orthovanadate (1 mM), and sodium fluoride (1 mM) were added to lysate buffer. SDS/PAGE (7–8%) was used for observation of phosphorylated Net1, and 16% SDS/PAGE was used for histones. After electrophoresis, proteins were transferred to nitrocellulose (Bio-Rad, Hercules, CA; 0.2 μM, cat. no. 162-0112). Antibodies were used as follows: PP-B, rabbit anti-phospho-Net1, (Azzam *et al.* 2004) 1:1,000 in 5% BSA-TBST; anti-FLAG (M2; Sigma-Aldrich, St. Louis, MO) 1:5000 in 3% milk-TBST; anti-H2B (Abcam, 1790) 1:1000 in 3% BSA-TBST; anti-H4 (Active Motif, 61199) 1:2000 in 5% BSA-TBST; anti-H3 (Abcam, 1791) 1:1000 in 5% milk-TBST; anti-H2A (Active Motif, 39236) 1:5000 in 3% BSA-TBST; and anti-H3-K9, K14ac (Upstate, 06-599) 1:10,000 in 5% milk-TBST. Anti-rabbit IgG and anti-mouse IgG HRP-conjugated secondary antibodies from Promega (Madison, WI; W4011 and W4021, respectively) were used at 1:10,000–1:20,000. Blots were developed with Pierce ECL Western Blot Substrate (ThermoScientific, 32106) and exposures obtained with Protein Simple FluorChem E imager. ImageJ was used to determine relative signal densities (Schneider *et al.* 2012).

RT-qPCR

The 20-ml cultures were grown to 1 O.D. A_{600} followed by hot phenol extraction of RNA (Lafon *et al.* 2012). After purification, RNA was treated with DNase (Ambion) followed by complementary DNA (cDNA) synthesis (TaqMan Reverse Transcriptase kit, Life Sciences). At least three independently prepared samples were evaluated for each comparison. Quantitative PCR (qPCR) was used to determine transcript levels relative to the *SCR1* control using EvaGreen qPCR Master Mix (Lamda Bio) on an MJ Research Opticon2. Oligonucleotides are listed in Table S3.

Data and reagent availability

All strains and plasmids listed in Table S1 and Table S2 that were generated in the L.P. lab are available upon request.

Results

Dosage suppressors of gcn5Δ temperature sensitivity: diverse roles for RTS1

We reported previously that overexpression of genes encoding Isw1 subunits can rescue the lethality observed upon loss of function of Gcn5 and Sas3, the two major H3 acetyltransferases in yeast (Lafon *et al.* 2012; Petty and Pillus 2013). To better understand these functionally overlapping acetyltransferases, we sought to identify gene dosage suppressors (reviewed in Rine 1991; Magtanong *et al.* 2011). We began by transforming the *gcn5*Δ *sas3-C357Y, P375A* temperature-sensitive mutant (Howe *et al.* 2001) with a 2μ library (Engebrecht *et al.* 1990) and screened 30,000 transformants for growth at the restrictive temperature. Suppressors were individually confirmed by dilution assays at high temperature and verified by isolating and retransforming the parental strain with recovered plasmids. Inserts of each suppressing plasmid were sequenced to identify its chromosomal fragment and each full-length gene within the fragment was individually subcloned to determine the suppressing factor. By this strategy, we isolated six distinct suppressors (Figure 1A), including *IOC2*, a subunit of the ISWI ATP-dependent chromatin remodeling complex (Lafon *et al.* 2012). The most frequently recovered suppressor was *RTS1*, which encodes a regulatory subunit of the PP2A complex. Four additional genes were identified a single time: *MED6*, *PAB1*, *RHO2*, and *ZDS1*. *MED6* encodes a subunit of the "head" module of the Mediator coactivator complex, *PAB1* encodes the major poly(A) binding protein in budding yeast, *RHO2* encodes one of several Rho-family GTPases, and *ZDS1* encodes a protein that binds $PP2A^{Cdc55}$ to promote cortical localization (Jonasson *et al.* 2016). Three of the originally isolated *RTS1* transformants along with several other suppressors are shown in Figure 1B.

We chose to pursue the mechanism of *RTS1* suppression of *gcn5*Δ *sas3-C357Y*, *P375A* as it was the most frequent hit from the screen and because genetic interactions between *GCN5-SAS3* and *RTS1* had not been previously described. Because *gcn5*Δ itself is temperature sensitive, it was important to determine whether rescue involved *SAS3*. To do so, we transformed *gcn5*Δ cells with the empty library vector, *RTS1*, or *IOC2*, to ask if *RTS1* rescue was *SAS3* independent. As we previously reported (Lafon *et al.* 2012), *IOC2* overexpression does not rescue *gcn5*Δ growth at high temperature; however, *RTS1* does (Figure 1C). Therefore, the *RTS1* suppressing mechanism is distinct from that of *IOC2*, and specific for *gcn5*Δ.

A

Gene	Description	Isolates
RTS1	B56 Regulatory subunit of PP2A	7
IOC2	Regulatory subunit of ISWI remodeling complex Isw1b	2
MED6	Core subunit of head module of RNAPII mediator complex	1
PAB1	PolyA-binding protein 1, part of the 3' end RNA-processinc complex	1
RHO2	Rho/Rac family GTPase, functions in cell polarity and microtubule assembly	1
ZDS1	Zillion different screens 1, regulates localization of Cdc55, Bcy1	1

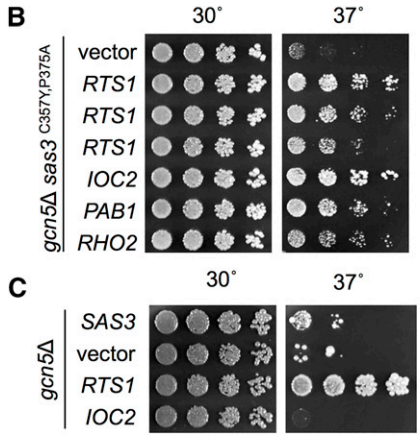

Figure 1 *RTS1* is a high-copy suppressor of *gcn5*Δ. (A) A screen for high-copy suppressors of *gcn5*Δ *sas3-C357Y, P375A* (LPY13321) lethality identified multiple independent isolates of *RTS1*. Suppression by *IOC2* has been characterized (Lafon *et al.* 2012). (B) Several of the independently isolated transformants identified in the dosage suppression screen that rescue *gcn5*Δ *sas3-C357Y, P375A* lethality at high temperature are shown. (C) Unlike *IOC2*, *RTS1* suppression of *gcn5*Δ (LPY10182) temperature sensitivity is independent of *SAS3*. Strains were grown on Leu$^-$ media for 3 days at indicated temperatures prior to imaging.

To characterize rescue of *gcn5*Δ by *RTS1*, we tested whether overexpression could suppress diverse phenotypes reported for *gcn5*Δ. These included DNA damage sensitivity, microtubule poison sensitivity, poor growth on nonfermentable carbon sources, delayed cell cycle progression, abnormal bud morphology, defects in sporulation, and osmotic stress sensitivity, as summarized in the *Saccharomyces* Genome Database (SGD) (Cherry *et al.* 2012). As shown in Figure 2A, the sensitivity of *gcn5*Δ to DNA damage-inducing agents HU and MMS was reduced upon *RTS1* overexpression. We used nocodazole to test for sensitivity to microtubule disruption and found that *RTS1* overexpression suppressed this phenotype (Figure 2B). *GCN5* mutants are unable to utilize nonfermentable carbon sources comparably to WT (Dimmer *et al.* 2002) and we found that *RTS1* overexpression improved growth with either glycerol or ethanol as a carbon source (Figure 2C). In order to determine if *RTS1* restored normal cell cycle control, we followed progression through S phase by flow cytometry in WT and *gcn5*Δ cells. We used α-factor to synchronize cultures in G1 and collected cells immediately and at 30 min after release. Upon release from α-factor, *gcn5*Δ cells did not progress into or through S phase as readily as WT. However, overexpression of *RTS1* suppressed this delayed entry into the cell cycle at both 30° and 37° (Figure 2D).

We did not observe rescue of *gcn5*Δ's bud morphology defect by *RTS1* overexpression (Figure S1A). In fact, overexpression of *RTS1* in both WT and *gcn5*Δ increased the frequency of abnormal budding. Additionally, diploids homozygous for *gcn5*Δ sporulate poorly with and without *RTS1* overexpression (Figure S1B). The fact that *RTS1* overexpression rescues stress-related phenotypes led us to test whether *RTS1* restored growth under osmotic stress conditions and whether general stress response transcription factors Hsf1, Hog1, Msn2, or Msn4 are required for *RTS1* rescue. We did not observe rescue of osmotic sensitivity (Figure S1C), nor did we find that *RTS1* rescue of temperature sensitivity required the stress response transcription factors (data not shown). Combined with the subset of phenotypes rescued by *RTS1* (summarized in Figure S1D), these results supported the idea that *RTS1* suppression was mediated through mechanisms distinct from general stress response pathways.

*PP2A^{Rts1} function is essential in gcn5*Δ *cells*

Rts1 is one of two regulatory PP2A subunits in budding yeast. The alternate regulatory subunit is encoded by *CDC55* (Figure 3A). Although *CDC55* was not recovered in the screen, to test specificity of suppression, we asked whether it rescued *gcn5*Δ growth similarly to *RTS1*. To do this, we compared growth of *gcn5*Δ transformed with a high-copy plasmid containing either *RTS1* or *CDC55* at high temperature. We found that *CDC55* overexpression did not rescue temperature sensitivity (Figure 3B). To further test the functional interactions between PP2A and Gcn5, we deleted the genes encoding each subunit of the PP2A complex in a *gcn5*Δ mutant and tested growth upon loss of a WT *GCN5* or *PPH22* plasmid by counterselection with 5-FOA. Loss of either *PPH21* or *PPH22* individually exacerbated *gcn5*Δ temperature sensitivity (data not shown), and loss of *CDC55* caused slow growth (Figure 3C). Most strikingly, we found that loss of Rts1, loss of the structural subunit Tpd3, or concurrent loss of both catalytic subunits Pph21 and Pph22 were lethal in *gcn5*Δ cells (Figure 3C, Figure S2A). Thus, PP2A^{Rts1} function is essential in *gcn5*Δ cells.

Because loss of *CDC55* can increase PP2A^{Rts1} formation (Bizzari and Marston 2011), we asked whether loss of *cdc55*Δ could suppress *gcn5*Δ temperature sensitivity. We compared *gcn5*Δ and *gcn5*Δ *cdc55*Δ growth at elevated temperatures (Figure S2B), but did not observe suppression similar to *RTS1* overexpression. We further evaluated the possibilities that the rescue of *gcn5*Δ growth by overexpression of *RTS1* could be due to reduced or altered PP2A^{Cdc55} activity. To test this possibility, we evaluated Net1, which is dephosphorylated by PP2A^{Cdc55} during mitosis to prevent early mitotic

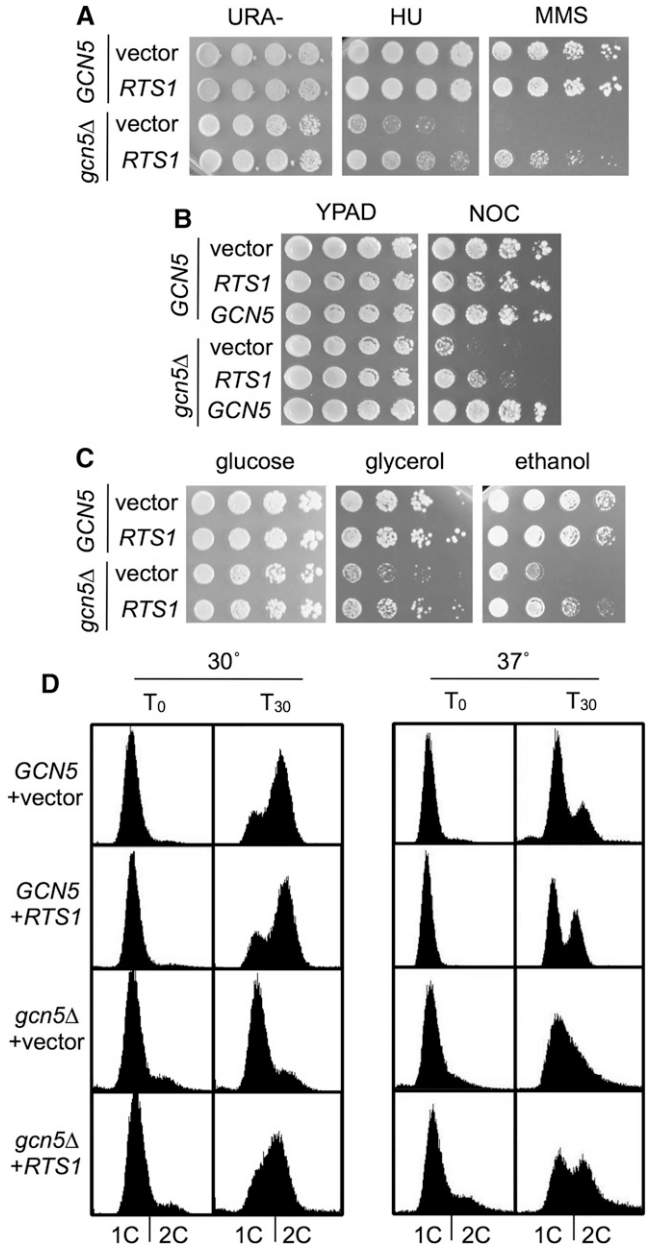

Figure 2 *RTS1* overexpression suppresses diverse *gcn5*Δ phenotypes. (A) *RTS1* overexpression rescues *gcn5*Δ growth on Ura$^-$ plates containing DNA damage inducers HU (0.1 M) and MMS (0.03%). (B) *RTS1* overexpression partially restores growth of *gcn5*Δ in the presence of microtubule destabilizing nocodazole (NOC) (2 μg/ml). (C) Growth on nonfermentable carbon sources glycerol and ethanol improves in *gcn5*Δ with *RTS1* overexpression. Cells were grown at 30° for 3 days (A and B) or 2 days (C). LPY5 (WT) and LPY10182 (*gcn5*Δ::*kanMX*) transformants are shown. (D) *RTS1* overexpression suppresses *gcn5*Δ slow progression into S phase. The *bar1*Δ (LPY11975) and *gcn5*Δ *bar1*Δ (LPY21272) transformants were arrested in G1 with pheromone α-factor at 30° for 90 and 120 min, respectively, and released into fresh medium for immediate collection (T_0) or to grow at 30° or 37° for 30 min prior to collection for flow cytometry. All data shown are representative of at least three independent experiments using independent transformants. See Figure S1 for additional analysis and summary.

exit (Queralt *et al.* 2006). We analyzed the levels of phosphorylated Net1 by immunoblotting whole cell lysates. We observed accumulation of the species recognized by the anti-Net1ph antibody PP-B (Azzam *et al.* 2004; Queralt *et al.* 2006) in *cdc55*Δ, but did not see a similar accumulation with *RTS1* overexpression (Figure S2C). These data suggested that the mechanism of *gcn5*Δ rescue by *RTS1* overexpression was not mediated by loss of PP2A^{Cdc55} activity.

OKA is a useful tool in analyzing phosphatase activity. It is a potent inhibitor of phosphoprotein phosphatase family enzymes (Swingle *et al.* 2007) with high affinity for both PP2A and the less abundant PP4, and lower affinity for PP1 and PP5 (Bialojan and Takai 1988; Haystead *et al.* 1989; Sasaki *et al.* 1994). Because of its high affinity and cell permeability, OKA has been used routinely to probe PP2A function. Specifically, Rts1 centromeric function was unaffected by OKA treatment, suggesting a mechanism independent of PP2A enzymatic activity (Peplowska *et al.* 2014). Further, PP2A subunit stoichiometry is reported to include three times as much Rts1 as Tpd3, the limiting subunit for PP2A complex assembly (Gentry and Hallberg 2002). These findings suggest independent functions for Rts1 beyond that of regulating PP2A phosphatase activity. We therefore sought to determine whether *RTS1*-mediated rescue required PP2A enzymatic function. Attempts to address this question genetically are precluded by the lethality of the *gcn5*Δ *pph21*Δ *pph22*Δ strain. Instead, we used OKA to determine if interrupting phosphoprotein phosphatase activity had an effect on *RTS1* rescue of *gcn5*Δ temperature sensitivity.

We treated cells grown to log phase at 30° with 10 μM OKA as described in Peplowska *et al.*, (2014) for 60 min, diluted ~2000 cells into fresh medium, and plated half of this dilution onto two plates, one prewarmed to 30°, the other to 36.5°. CFUs were counted to evaluate growth at 36.5° relative to 30°. As shown in Figure 3D, temporary inhibition of phosphoprotein phosphatase activity by OKA dampened rescue of *gcn5*Δ growth by *RTS1* overexpression. These results support the hypothesis that *RTS1* rescue is mediated through the PP2A^{Rts1} complex, but do not exclude the possibility that other phosphatases, such as PP4, may also contribute to rescue.

RTS1 functionally interacts with the SAGA complex

Gcn5 is a subunit of multiple complexes: the transcriptional coactivator SAGA, the retrograde pathway-specific SLIK/-SALSA, and the less well-characterized ADA complex (Figure 4A) (Grant *et al.* 1997; Eberharter *et al.* 1999; Sterner *et al.* 2002; Lee *et al.* 2011). To determine whether PP2A^{Rts1} was linked to a specific Gcn5-containing complex, we constructed double mutants with genes encoding representative members of modules distinguishing the complexes.

Components tested included Spt20, an architectural subunit of SAGA, necessary for complex assembly (Roberts and Winston 1996; Sterner *et al.* 1999; Lee *et al.* 2011), and both ADA-specific complex subunits Ahc1 and Ahc2 (Eberharter *et al.* 1999; Lee *et al.* 2011). We also tested the interaction between *RTS1* and the only SLIK/SALSA-specific subunit gene, *RTG2* (Pray-Grant *et al.* 2002). We observed synthetic lethality between *rts1*Δ and *spt20*Δ as well as *gcn5*Δ, but not

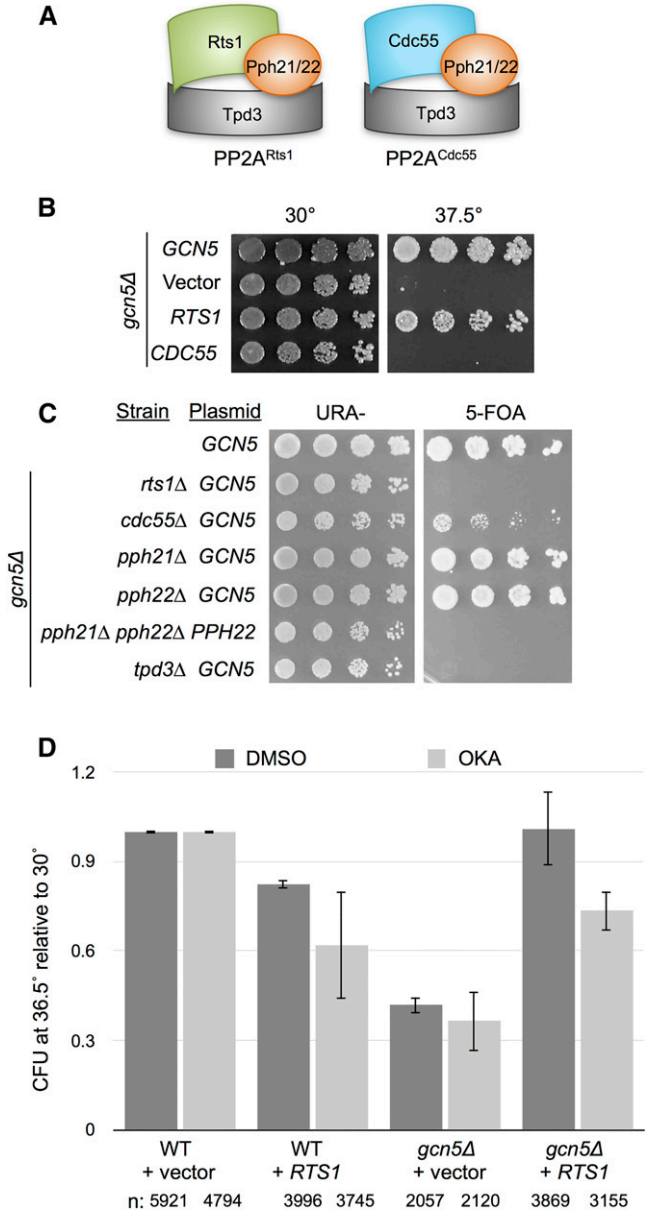

Figure 3 Loss of PP2A^{Rts1} function impairs growth and *RTS1* rescue in *gcn5*Δ. (A) Cartoon representations of two yeast PP2A complexes are adapted from crystal structures (Cho and Xu 2007). (B) Only *RTS1* overexpression, not *CDC55*, can suppress *gcn5*Δ temperature sensitivity. LPY10182 (*gcn5*Δ::*kanMX*) was transformed with 2μ *GCN5* (pLP1524), empty vector (pLP135), *RTS1* (pLP2197), and *CDC55* (pLP2330). Fresh transformants were grown overnight and plated onto Leu$^-$ medium prewarmed to the indicated temperature, and grown for 4 days. (C) Loss of PP2A^{Rts1} is lethal in *gcn5*Δ. WT (LPY5), *gcn5*Δ *rts1*Δ (LPY15178), *gcn5*Δ *cdc55*Δ (LPY15178), *gcn5*Δ *pph21*Δ (LPY15296), *gcn5*Δ *pph22*Δ (LPY14692), *gcn5*Δ *pph21*Δ *pph22*Δ (LPY20694), and *gcn5*Δ *tpd3*Δ (LPY15416) are all shown transformed with pLP1640 (*GCN5*). The *gcn5*Δ *pph21*Δ *pph22*Δ mutant (LPY20694) was transformed with pLP2997 (*PPH22*). Cells were plated onto Ura$^-$ and 5-FOA to select against the *GCN5* or *PPH22* CEN plasmid and grown for 3 days at 30°. (D) Treatment with the phosphoprotein phosphatase inhibitor OKA reduces *RTS1* suppression of *gcn5*Δ temperature sensitivity. Log-phase cells were treated with 10 μM OKA or DMSO (control) for 1 hr prior to plating onto Ura$^-$ plates prewarmed to 30° or 36.5°. OKA treatment caused temperature sensitivity in WT cells when grown at 37° (not shown), so a slightly lower temperature was used for this assay. Cells were grown for 3 days prior to counting CFUs on each plate. Survival at high temperature was determined by calculating the ratio of CFUs at 36.5° to 30° followed by normalization to WT + vector controls, where *n* indicates total CFUs counted in three experiments for each transformant, and the error bars show standard deviation. See Table S4 for all normalized relative survival ratios.

between *rts1*Δ and the ADA-specific mutants nor with the SLIK/SALSA-specific *rtg2*Δ mutant (Figure 4B, Figure S3A). To determine if lethality was due to loss of Gcn5 catalytic activity, we expressed two well-characterized *GCN5* HAT mutants in a plasmid shuffle in *gcn5*Δ *rts1*Δ cells. Of the two mutants, *GCN5-LKN* and *GCN5-KQL*, the latter is catalytically inactive (Wang *et al.* 1998; Grant *et al.* 1999). Whereas expression of *GCN5-LKN* supported viability, expression of *GCN5-KQL* did not (Figure S3B). Thus, Gcn5 catalytic function is essential in *rts1*Δ cells.

Because SAGA and SLIK/SALSA include distinct functional modules (Sterner *et al.* 1999; Wu *et al.* 2004; Lee *et al.* 2011), we further dissected the genetic interaction between *RTS1* and two of the modules. Among these, *SPT8* encodes a SAGA-specific subunit that mediates the physical and functional interaction between the complex and TATA-binding protein (TBP) (Eisenmann *et al.* 1994; Warfield *et al.* 2004) and *UBP8* encodes the deubiquitinase enzyme of the DUB module that removes H2B-K123 monoubiquitylation (Henry *et al.* 2003). Whereas previous high-throughput epistatic miniarray profile analysis found an increase in relative fitness of *rts1*Δ *spt8*Δ double mutants (Collins *et al.* 2007), we observed synthetic sickness in the *rts1*Δ *spt8*Δ mutant. This discrepancy may be due to the different genetic background used for the two studies or the difference in comparing growth of single colonies to growth of populations derived from single colonies in the dilution assays shown. Regardless, the interaction we observe is not as severe as with *SPT20* or *GCN5* deletion. We also found that deletion of the DUB-specific gene *UBP8* had little effect on *rts1*Δ growth. This observation is consistent with the fact that loss of Spt20 does not strongly affect DUB function (Henry *et al.* 2003) and, combined, suggests that the functional interaction of *RTS1* with SAGA and SLIK/SALSA is DUB independent.

Loss of *SPT20*, *SPT8*, or *UBP8* sensitizes cells to various stresses (SGD, Cherry *et al.* 2012). We tested whether *RTS1* overexpression could suppress *spt20*Δ, *spt8*Δ, and *ubp8*Δ temperature and MMS sensitivity as for *gcn5*Δ. We found that overexpression of *RTS1* indeed improved growth of *spt20*Δ and *spt8*Δ at high temperatures and improved growth of all SAGA single mutants on MMS (Figure 4C). Together, these results support the idea that the catalytic activity of Gcn5 interacts with PP2A^{Rts1} as part of the SAGA and/or SLIK/SALSA complexes.

A major function of Gcn5 as a member of the SAGA and SLIK/SALSA complexes is acetylation of histone H3 to activate transcription. Gcn5 targets H3 predominantly at lysines 9 and 14 (K9, K14) and loss of Gcn5 has a global impact on

levels of these marks *in vivo* (Zhang *et al.* 1998; Howe *et al.* 2001; Pray-Grant *et al.* 2005; Downey *et al.* 2015).

We asked if *RTS1* mediated restoration of H3 acetylation. In *gcn5*Δ cells overexpressing *RTS1*, we observed a reproducible increase in global H3-K9, K14ac (Figure 4D), as quantified in Figure 4E. We then asked whether the increase in H3 acetylation correlated with higher transcription of Gcn5-regulated genes. We selected four highly expressed genes previously identified as Gcn5 regulated (Huisinga and Pugh 2004) for RT-qPCR analysis. We collected cells grown to log phase under suppressing conditions and measured expression of the selected genes relative to *SCR1*, an RNA polymerase III-transcribed gene. Increased expression was not observed in cells overexpressing *RTS1* (Figure S3C). This result suggested that the mechanism of *gcn5*Δ rescue by *RTS1* was not via global restoration of Gcn5-dependent gene expression.

RTS1 overexpression restores histone gene expression in gcn5Δ cells

We considered that the increase in relative H3 acetylation observed in *gcn5*Δ cells overexpressing *RTS1* could be due to increased activity of another HAT, decreased activity of an HDAC such as Hda1 or Sir2, or an increase in overall H3 in the cell. We were intrigued by the third possibility, as *RTS1* had previously been found to promote cell-cycle-regulated gene expression (Artiles *et al.* 2009; Parnell *et al.* 2014; Zapata *et al.* 2014) and *RTS1* overexpression suppressed *gcn5*Δ's slow G1–S progression (Figure 2D). To test a role in histone expression, we quantified unmodified H3 levels along with the other core histones in WT and *gcn5*Δ by immunoblotting and found that *gcn5*Δ cells had reduced levels of core histones compared to WT (Figure S4, A and B). Further, *RTS1* overexpression restored levels of all histones (Figure S4, A and B).

Unlike other eukaryotes where there are several copies of each canonical histone gene, there are only two genes for each in *Saccharomyces cerevisiae*. Histone gene loci in budding yeast contain pairs of histone genes oriented in opposite directions from a shared promoter, and each pair is coordinately regulated and expressed (Eriksson *et al.* 2012). Analysis of Gcn5 (Venters *et al.* 2011), and H3-K9, K14ac genome-wide chromatin immunoprecipitation data (Pokholok *et al.* 2005) revealed that Gcn5 and H3-K9, K14ac are found at the promoters of each histone gene pair. Additionally, genomic expression analysis in *gcn5*Δ and *gcn5-KQL* mutants showed reduced histone expression (Huisinga and Pugh 2004). To determine if the changes in global histone protein levels we observed in *gcn5*Δ were regulated at the level of transcription, we quantified RNA prepared from logarithmically growing cells by RT-qPCR. All histone genes have significantly reduced expression in *gcn5*Δ, with the notable exception of *HTA1*, which did not show any significant changes (Figure 5A). To our knowledge this is the first report of divergent rather than coordinate regulation of gene expression at the *HTA1-HTB1* locus. Similar to protein levels, *RTS1* overexpression also restored histone mRNAs to near WT levels (Figure 5A).

As in other eukaryotes, yeast histone gene expression is tightly regulated in a cell-cycle-dependent manner. Histone genes are turned on at the end of G1 in preparation for genome replication and turned off at the end of S phase (Eriksson *et al.* 2012). To evaluate the effects *GCN5* loss and overexpression of *RTS1* on cell-cycle-regulated histone gene induction, we arrested cells in G1 with α-factor and collected samples for RNA extraction at 20-min intervals after release into S phase. We observed similar levels of *HTA1* expression in WT and *gcn5*Δ, independently of *RTS1* overexpression (Figure 5B). This finding was consistent with our observation in asynchronous cultures that *HTA1* expression was unaffected by loss of *GCN5* or overexpression of *RTS1*. By contrast, there was decreased induction of *HTB1* expression in *gcn5*Δ cells. This decrease was rescued in cells overexpressing *RTS1*. Thus, Gcn5 was an important positive regulator of histone gene expression. Further, our results suggested that *RTS1*-dependent suppression of *gcn5*Δ was, in part, mediated through histone gene expression.

Does RTS1 suppression require specific histone residues?

Dynamic histone phosphorylation is a key regulator of chromatin-templated functions (Banerjee and Chakravarti 2011; Rossetto *et al.* 2012; Zentner *et al.* 2013; Sawicka and Seiser 2014; Tessarz and Kouzarides 2014). Many kinases targeting histones continue to be discovered and characterized, but much less is known of the phosphatases responsible for removing this modification. We hypothesized that the $PP2A^{Rts1}$–Gcn5 interaction was mediated through dynamic modification of specific histone residues. We first tested whether well-characterized sites of histone phosphorylation were required for *RTS1* suppression of *gcn5*Δ temperature sensitivity. Among these, H3-S10ph functions in chromosome condensation in mitosis and meiosis (Johansen and Johansen 2006). Phosphorylation at this site also has reported crosstalk with H3-K9 and K14 acetylation (Cheung *et al.* 2000; Lo *et al.* 2000; Edmondson *et al.* 2002). Histone H3-S28ph is linked to H3-S10ph and is associated with transcriptional response to stress in mammalian cells (Clayton and Mahadevan 2003; Sawicka *et al.* 2014). Histone H3-T45ph functions during DNA replication (Baker *et al.* 2010), and, lastly, H2A-S121ph has a role in DNA damage and protection of centromeric cohesion in budding yeast (Fernius and Hardwick 2007; Moore *et al.* 2007).

Mutation of H3-S10 to alanine did not interfere with *RTS1* rescue (Figure S5A). Further, loss of an H3-S10 kinase Snf1 did not interfere with *RTS1* rescue (data not shown), consistent with a lack of function for this modification in the interaction. Similarly, mutation at H3-S28, H3-T45, and H2A-S121 did not impair rescue by *RTS1* (Figure S5A).

We continued to test the hypothesis that histone phosphorylation underlies the *RTS1–GCN5* interaction. Using an unbiased approach, we tested the scanning histone mutagenesis with alanine (SHIMA) library (Nakanishi *et al.* 2008) to screen all serine and threonine residues (Figure 6A) for effects on

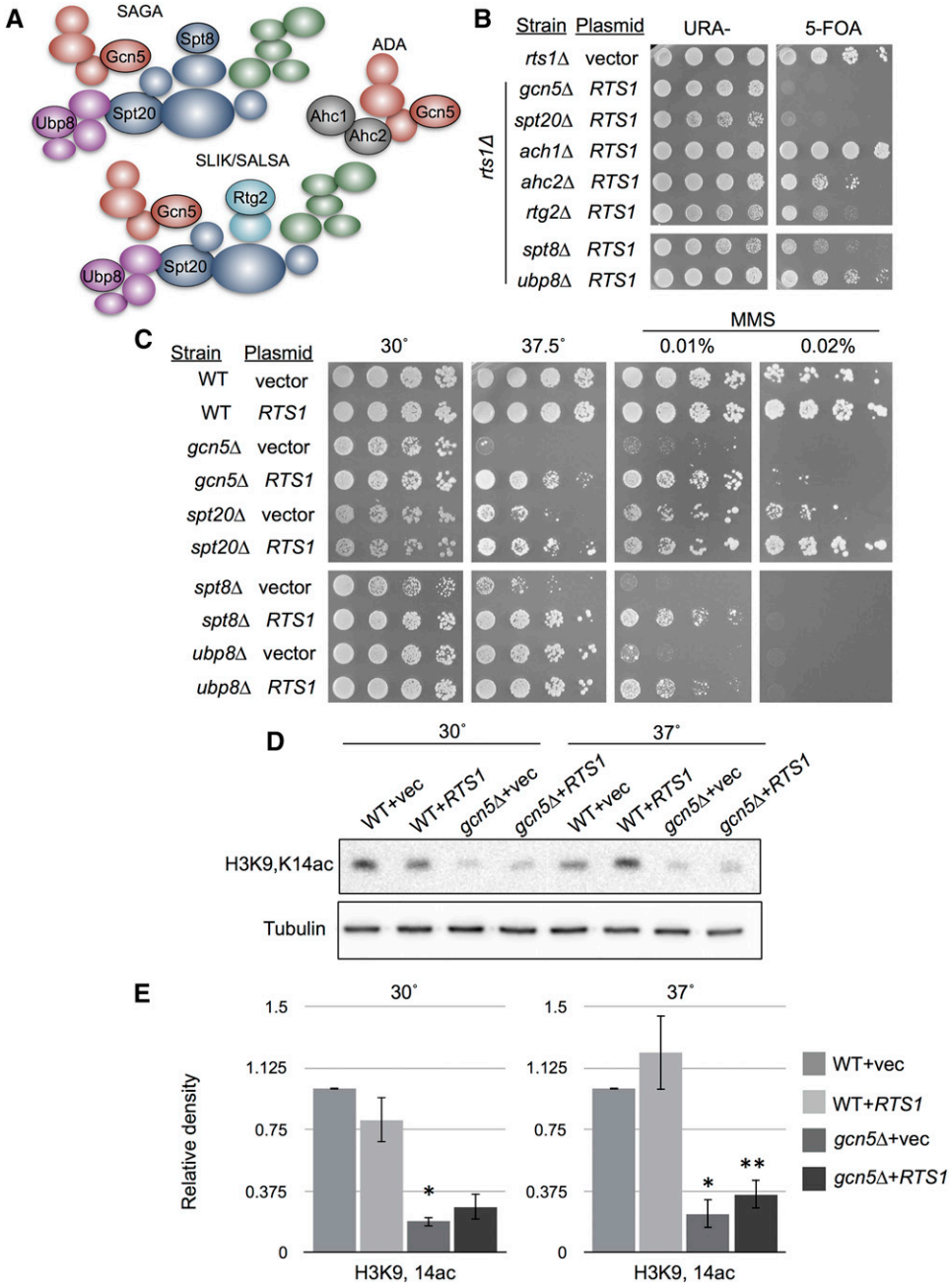

Figure 4 There is a functional interaction between *RTS1* and SAGA. (A) Molecular models of three Gcn5-containing complexes in budding yeast (Lee *et al.* 2011). (B) Genetic analysis of *rts1*Δ (LPY14653) with SAGA, ADA, and SLIK/SALSA subunits highlighted by black outlines. The *rts1*Δ strain was transformed with *RTS1-URA3* (pLP2462) and crossed to generate the double mutants shown. Strains were plated onto Ura$^-$ (growth) and 5-FOA to select against the *RTS1* plasmid and grown for 3 days at 30°. Synthetic lethality is observed with *rts1*Δ *gcn5*Δ (LPY15178) and *rts1*Δ *spt20*Δ (LPY17484) but not with loss of ADA subunits encoded by *AHC1* (LPY18424), *AHC2* (LPY18495), or the SLIK/SALSA-specific *RTG2* (LPY20692). Deletion of the SAGA-specific *SPT8* (LPY21898), encoding a TBP-binding subunit, and *UBP8* (LPY21081), encoding the deubiquitinase subunit, are also viable in *rts1*Δ. (C) *RTS1* improves *gcn5*Δ (LPY10182), *spt20*Δ (LPY16914), and *spt8*Δ (LPY6487) growth at high temperature and in DNA damaging conditions in all strains shown, including *ubp8*Δ (LPY8240). Strains were transformed with vector or *RTS1* and plated onto Ura$^-$ plates with and without MMS and grown for 3 days at 30° or 37.5° as indicated. (D) *RTS1* overexpression results in increases in H3-K9, K14ac. Log-phase cells grown at indicated temperature were collected for protein lysate preparation; shown is a representative immunoblot. (E) Quantification of relative H3-K9, K14ac signal from three biological replicates is shown. Error bars indicate standard deviation. Asterisks indicate *P*-values <0.05 by paired Student's *t*-test: a single asterisk indicates significant difference compared to WT + vector and a double asterisk, compared to *gcn5*Δ + vector. All normalized averages and significant *P*-values are listed in Table S4.

RTS1 rescue of temperature sensitivity. Briefly, we constructed a *gcn5*Δ strain that also lacked chromosomal copies of the core histones. To maintain viability, the strains contain a *URA3*-plasmid bearing a copy of each core histone pair. We then transformed a histone plasmid bearing a single alanine substitution of each of the 72 nonessential serine or threonine residues (H3-T118A is lethal) (Nakanishi *et al.* 2008). We then selected for loss of the WT plasmid using 5-FOA and tested for effects on rescue by *RTS1* overexpression.

Although PP2A^{Rts1} is classified as a serine/threonine phosphatase, we also considered three tyrosine residues that have been identified as phosphorylated in phosphoproteomic studies: Y40, Y43, and Y45 on histone H2B (PhosphoGRID). Previous work identified H2B-Y40 phosphorylation by the Wee1 kinase (Swe1) as an important regulator of histone gene expression in budding yeast and human cells (Mahajan *et al.* 2012; Mahajan and Mahajan 2013). A recent study has linked PP2A^{Rts1} with *in vivo* dephosphorylation of tyrosine 19 of Cdk1, another Swe1 substrate (Kennedy *et al.* 2015). We constructed the structurally conservative tyrosine-to-phenylalanine substitutions for the H2B tyrosine residues of interest and transformed into the histone shuffle strains as above.

Two residues of H2B are required for *RTS1* overexpression to rescue *gcn5*Δ temperature sensitivity: Y40 and T91 (Figure 6, B and C). Mutation to neighboring residues Y43 and S90

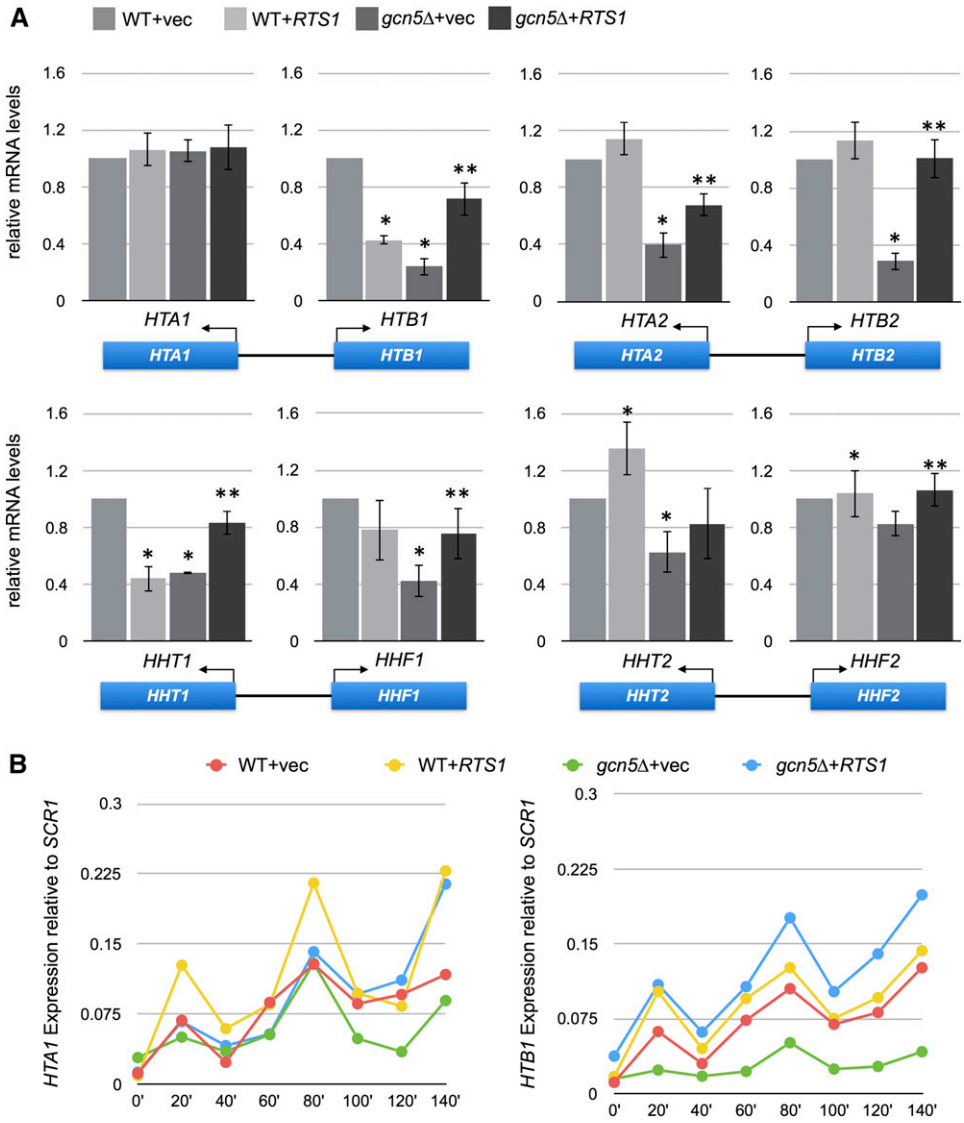

Figure 5 *RTS1* overexpression restores histone gene expression in asynchronous *gcn5*Δ populations. (A) RT-qPCR analysis of histone mRNA reveals lower histone gene expression in *gcn5*Δ at 37° relative to the RNA Pol III transcript, *SCR1*, except for *HTA1*, which revealed no significant change. Gene expression increased with *RTS1* overexpression, except for *HHT2*. Error bars indicate standard deviation from three independent experiments using fresh 2μ vector (pLP136) and *RTS1* (pLP2462) transformants derived from LPY5 (WT) and LPY10182 (*gcn5*Δ::*kanMX*). Asterisks indicate *P*-values <0.05 by paired Student's *t*-test: a single asterisk indicates significant difference compared to WT + vector and a double asterisk, compared to *gcn5*Δ + vector. All normalized averages and significant *P*-values are listed in Table S4. Each histone gene pair locus is diagrammed below the corresponding histograms. Oligonucleotide sequences for qPCR amplification of all histone genes except for *HHF2* were originally published in Mahajan *et al.* (2012). (B) *RTS1* overexpression restores *HTB1* expression upon release from α-factor arrest. Early log-phase transformants of WT (LPY11975) and *gcn5*Δ (21272) were arrested with α-factor at 30° and samples were taken every 20 min upon release to grow at 37° for RT-qPCR analysis. *HTA1* induction is similar, but *HTB1* induction is reduced in between *gcn5*Δ and WT. This difference is suppressed when *RTS1* is overexpressed.

did not impair rescue, demonstrating that loss of growth is specific to T91 and Y40. Further, the *htb1-T91A* and htb1-Y40F mutations prevented *RTS1* rescue of HU and MMS sensitivity, and htb-T91A also impaired restored growth by *RTS1* on nocodazole (Figure 6D). These results suggested overlapping but distinct functions for the two H2B residues in *RTS1* rescue of *gcn5*Δ: both are important for rescue of DNA damage and replication stress, but T91 is more important for rescue of mitotic stress. The Y40 and T91 residues are found on the lateral surface of the core nucleosome structure in close proximity to the surrounding DNA (Figure 6B), and neither the Y40F mutation nor the T91A mutation led to decreased H2B, so the effects are not likely due to gross instability of H2B caused by the site mutations (Figure S5B). The changes in histone gene dosage in the histone shuffle mutants used for this study prevent analysis of expression of each histone gene; however, we did ask whether *htb1-Y40F* and *htb1-T91A* mutations affect global H3 acetylation. Although the quantitative data were not statistically significant, we observed a consistent reduction in global H3 acetylation in *gcn5*Δ *htb1-Y40F* and *htb1-T91A* mutants overexpressing *RTS1* (Figure S5C).

Mutation of H2B-T91 supports a role for dynamic modification

H2B-T91 has not been characterized in yeast, although the corresponding residues of human and mouse H2B have been identified as phosphorylated by mass spectrometry (Cell Signaling Technology, phosphosite.org). For further functional analysis, we generated mutations of H2B-T91 to aspartic acid (D) or glutamic acid (E), whose structures are similar to phosphothreonine. The phosphomimetic mutants impaired growth in the WT strain and were lethal in *gcn5*Δ (Figure 7A, Figure S6A). We determined whether expression of H2B was altered by the phosphomimetic mutations in *GCN5* cells, and found that *htb1-T91D* reduced levels, likely resulting in the reduced growth of this strain compared to *htb1-T91E* (Figure S6B). Finally, we tested whether *RTS1* overexpression improved growth of the phosphomimetic mutant strains, but

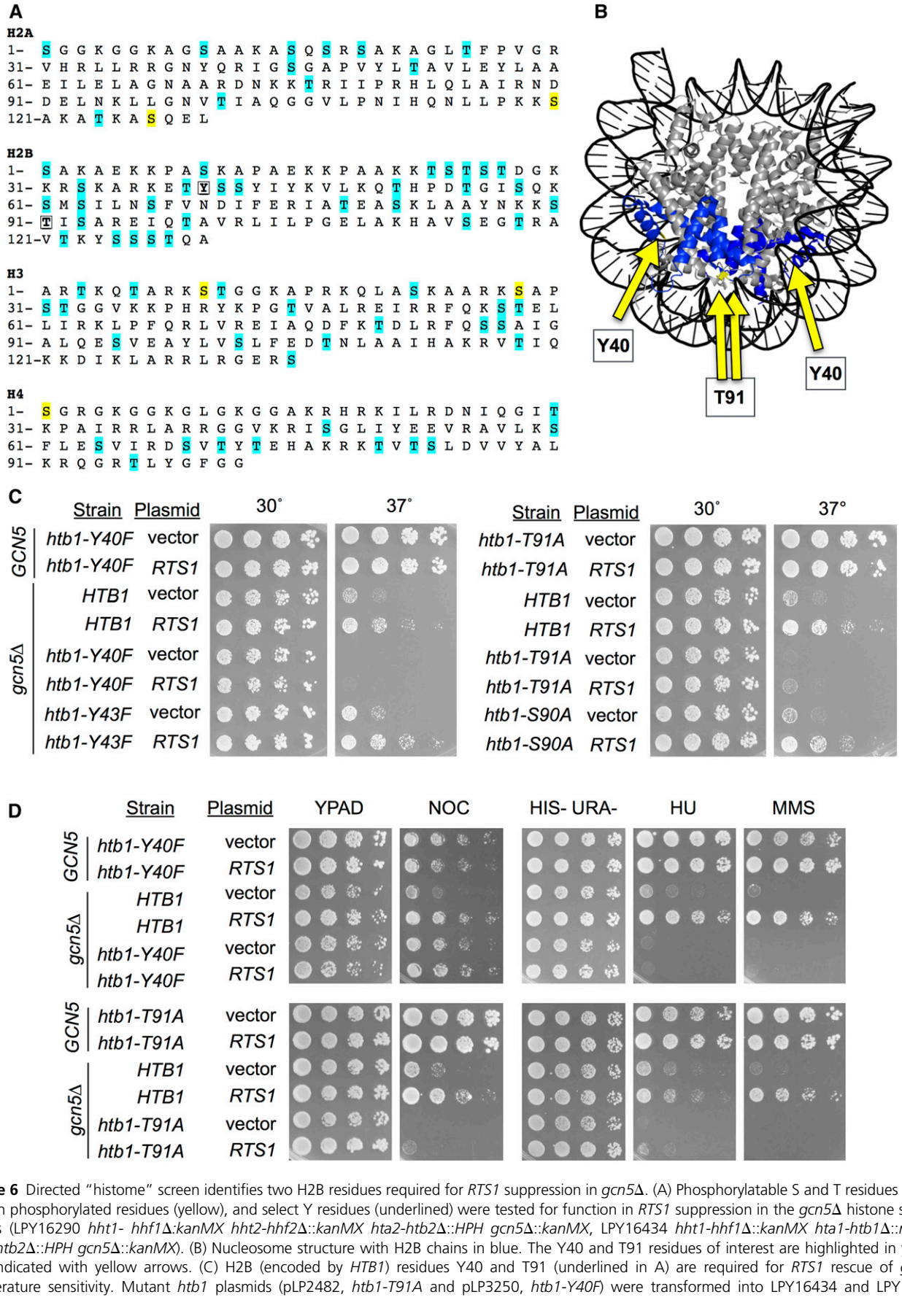

Figure 6 Directed "histone" screen identifies two H2B residues required for *RTS1* suppression in *gcn5*Δ. (A) Phosphorylatable S and T residues (blue), known phosphorylated residues (yellow), and select Y residues (underlined) were tested for function in *RTS1* suppression in the *gcn5*Δ histone shuffle strains (LPY16290 *hht1- hhf1*Δ*:kanMX hht2-hhf2*Δ*::kanMX hta2-htb2*Δ*::HPH gcn5*Δ*::kanMX*, LPY16434 *hht1-hhf1*Δ*::kanMX hta1-htb1*Δ*::natMX hta2-htb2*Δ*::HPH gcn5*Δ*::kanMX*). (B) Nucleosome structure with H2B chains in blue. The Y40 and T91 residues of interest are highlighted in yellow and indicated with yellow arrows. (C) H2B (encoded by *HTB1*) residues Y40 and T91 (underlined in A) are required for *RTS1* rescue of *gcn5*Δ temperature sensitivity. Mutant *htb1* plasmids (pLP2482, *htb1-T91A* and pLP3250, *htb1-Y40F*) were transformed into LPY16434 and LPY14461

only observed a very slight growth improvement for the *GCN5* strain and no rescue of lethality in *gcn5*Δ (Figure 7B). Thus, dynamic modification of H2B at threonine 91 is important for cell growth and essential in the absence of Gcn5.

Discussion

We report six dosage suppressors of conditional lethality in *gcn5*Δ *sas3-C357Y,P375A* mutants. Among these, we have demonstrated robust interactions between the Gcn5-containing SAGA and SLIK/SALSA complexes and PP2A^{Rts1} in the regulation of growth and histone gene expression. We identified *RTS1* as a high-copy suppressor of a specific subset of *gcn5*Δ phenotypes: temperature and DNA damage sensitivity, poor growth on nonfermentable carbon sources, and slow cell cycle entry upon release from G1 arrest. Conversely, loss of PP2A^{Rts1} was lethal in *gcn5*Δ cells or those expressing catalytically inactive Gcn5. Genetic dissection demonstrated that it is loss of SAGA and/or SLIK/SALSA function that results in synthetic lethality with loss of PP2A^{Rts1}.

We found that *gcn5*Δ had a defect in histone expression at the level of transcription in both asynchronous and synchronized populations and in cellular levels of histone proteins. *RTS1* overexpression restored histone expression to WT levels. A screen of phosphorylatable residues of the core histones revealed that rescue by *RTS1* required two residues of H2B, Y40, and T91. Phosphomimetic mutants of T91 caused sickness in WT and lethality in *gcn5*Δ, suggesting that regulating dynamic phosphorylation at this site is important for growth and becomes critical with loss of Gcn5. H2B-Y40ph was previously reported to function in regulation of gene expression (Mahajan *et al.* 2012; Mahajan and Mahajan 2013).

Several studies have reported synthetic interactions between *GCN5* and histone genes. For example, semidominant *sin* alleles of *HHT2* and *HHF2* can restore reporter gene expression in *gcn5*Δ cells (Pollard and Peterson 1997). Additionally, deletion of the N-terminal tails of H3 or H4, H3-K14R, H3-R17A, and H4-K8R, K-16R mutations are lethal in cells lacking Gcn5 (Zhang *et al.* 1998; Ruault and Pillus 2006). Beyond these interactions, we demonstrate loss of *GCN5* causes a specific defect in histone gene expression. It is possible that H2B-Y40 is particularly important for turning off histone gene expression at the end of S phase upon overexpression of *RTS1* (Mahajan *et al.* 2012; Mahajan and Mahajan 2013), to prevent cytotoxicity caused by elevated histone expression (Meeks-Wagner and Hartwell 1986; Singh *et al.* 2010). Consistent with a central role in histone gene expression is the synthetic lethality observed upon loss of the individual SAGA subunits Spt8, Spt20, and Gcn5 with deletion of the histone transcriptional activator Spt10 (Chang and Winston 2013). Normal cell cycle progression and DNA repair require precise regulation of histone levels (Singh *et al.* 2009; Singh *et al.* 2010; Eriksson *et al.* 2012; Liang *et al.* 2012; Ghule *et al.* 2014), therefore restoration of histone expression likely contributes to the restored cell cycle progression and growth upon DNA damage that we observe in *gcn5*Δ cells overexpressing *RTS1*.

At the end of S phase, Wee1 phosphorylates H2B-Y40 at histone gene promoters to downregulate expression (Mahajan *et al.* 2012), but a counteracting phosphatase is unknown. Future work should determine whether PP2A^{Rts1} directly dephosphorylates H2BY40ph as part of the mechanism of histone gene activation. Although PP2A is classified as a serine/threonine phosphatase, its dephosphorylation of tyrosine residues has been reported *in vitro* (Cayla *et al.* 1990) and recently proposed *in vivo* (Kennedy *et al.* 2015). We predict that if PP2A^{Rts1} directly dephosphorylates H2BY40ph, it does so in a manner regulated by cell cycle cues.

Alternatively, the mechanism by which *RTS1* modulates proper histone gene expression may be less direct. Loss of Gcn5 reduces binding of the G1-specific cell cycle transcription factor SBF to the *HO* promoter, resulting in reduced expression (Cosma *et al.* 1999; Krebs *et al.* 1999). The SBF transcription factor complex also promotes histone gene expression in late G1 (Eriksson *et al.* 2012). Therefore, a mechanism may involve PP2A^{Rts1} promoting cell-cycle-regulated transcription through SBF or other G1 activators as reported previously for the G1 cyclin Cln3 (Artiles *et al.* 2009; Parnell *et al.* 2014; Zapata *et al.* 2014) or negative regulation of a repressor similar to that reported for Ash1 (Parnell *et al.* 2014). Indeed, Swi4, the DNA-binding subunit of SBF, was found to be hyperphosphorylated in *rts1*Δ cells (Zapata *et al.* 2014). PP2A^{Rts1} activation of histone gene expression may therefore be achieved in part by regulating Swi4 phosphorylation.

A distinct mechanism of *RTS1* rescue may be mediated through H2B-T91. The phosphomimetic mutant phenotypes suggest that T91, like Y40, is a site of dynamic phosphorylation. Of note, *htb1-T91E* overexpressing empty vector or *RTS1* grew poorly upon loss of the covering plasmid (compared to Figure 7A and Figure S6A), suggesting that the 2μ plasmids exacerbated sickness or that the more robust growth of *htb1-T91E* observed in Figure 7A and Figure S6A was due to growth of suppressors arising from recombination of *HTB1* from the covering plasmid. In either case, a state mimicking constitutive H2B T91 phosphorylation is clearly detrimental to cell growth.

The residue homologous to H2B-T91 in mammals (H2B-T89) is phosphorylated in murine brain and human cancer cells (phosphosite.org). The kinase prediction program GPS 2.0 (Xue *et al.* 2008) identifies the kinases Ste20 and Rad53

(*hht1-hhf1*Δ::*kanMX hta1-htb1*Δ::*natMX hta2-htb2*Δ::*HPH*) containing *RTS1* or vector control high-copy plasmids. 5-FOA was used to select against the WT histone plasmid from these strains before plating onto His$^-$ Leu$^-$ media as shown and grown for 3 days at the indicated temperature. (D) H2B-Y40 and T91 are required for *RTS1* rescue of DNA damage sensitivity (0.05 M HU, 0.02% MMS). H2B-T91 is also required for *RTS1* rescue of sensitivity to microtubule destabilization by NOC (2 μg/ml). Fresh histone mutant transformants were generated as above before plating and grown for 3 days at 30°.

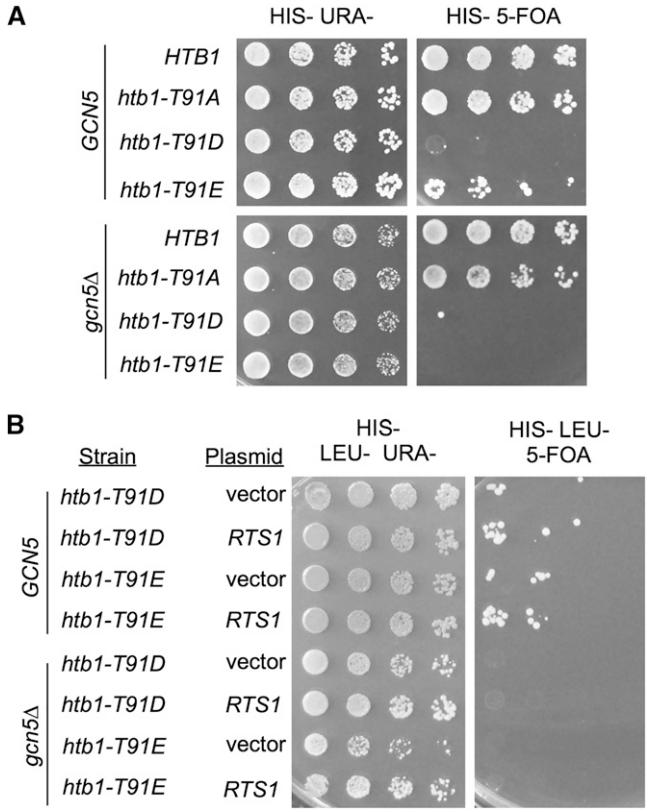

Figure 7 HTB1-T91 dynamic modification is essential for growth. (A) Phosphomimetic mutation of T91 is lethal in *gcn5*Δ and causes slow growth in *GCN5* cells. Site-directed mutagenesis was used to mutate *htb1-T91A* to D/E to generate pLP2689 and 2770 and transformed into LPY16434 and LPY14461 histone shuffle strains. (B) *RTS1* overexpression does not rescue slow growth and lethality caused by *htb1-T91D/E* phosphomimetic mutations. Transformants were plated onto His^- Ura^- or His^- Leu^- Ura^- (growth) and 5-FOA to select against the WT histone plasmid as shown and grown for 3 days at 30°.

as candidates for H2B-T91 phosphorylation, both of which have documented histone phosphorylation activity. Ste20 phosphorylates H2B-S10 during peroxide-induced cell death in budding yeast (Ahn *et al.* 2005a,b) and histone phosphorylation by Rad53 is involved in ubiquitin-mediated degradation to prevent excess histone levels (Gunjan and Verreault 2003; Singh *et al.* 2009). The slight increase in H2B observed in the *gcn5*Δ *htb1-T91A* cells at 30° (Figure S5B) might therefore be due to reduced Rad53-driven proteolysis.

We note that *RTS1* overexpression affected growth and gene expression in otherwise WT cells in several experiments. WT cells overexpressing *RTS1* have reduced high-temperature survival after temporary phosphoprotein phosphatase inhibition by OKA (Figure 3D), suggesting that in the absence of phosphatase activity, *RTS1* overexpression can impair growth under stress conditions. *RTS1* overexpression also slightly improved growth of WT cells exposed to MMS (Figure 4C), supporting a role for *RTS1* in the DNA damage response. WT cells overexpressing *RTS1* also exhibited noteworthy changes in gene expression and histone levels compared to the empty vector controls (Figure 5, A and B, Figure S3C, Figure S4). In asynchronous populations, we observed 57, 56, and 22% lower relative expression of *HTB1*, *HHT1*, and *HHF1*, respectively, and 36% increase in *HHT2* expression (Figure 5A). In synchronized cells, *RTS1* overexpression increased *HTA1* induction (Figure 5B). We observed 20% more H3 and 50% less H4 in WT asynchronous cells overexpressing *RTS1* (Figure S4), consistent with some of the changes observed for mRNA levels. Combined, these results support a role for *RTS1* in regulation of cellular histone levels. When testing the panel of highly expressed *GCN5*-regulated genes, we found significant changes in expression, particularly of *GPG1* and *PHM8* (117 and 68% increases in expression, respectively). Both *GPG1* and *PHM8* are upregulated by the transcription factor Haa1, which relocalizes to the nucleus upon weak acid stress and in conditions of DNA replication stress (Tkach *et al.* 2012; Sugiyama *et al.* 2014). Coincident with Haa1 nuclear accumulation is loss of phosphorylation (Sugiyama and Nikawa 2001), but the phosphatase has not yet been identified. Our data are consistent with the possibility that Haa1 phosphorylation is regulated by $PP2A^{Rts1}$, leading to activation of target genes. Finally, although not statistically significant, we observed changes in global H3 acetylation in *RTS1* overexpressing cells (Figure 4, D and E). Combined with the functional interaction between *RTS1* and *GCN5* we have characterized in detail, we propose $PP2A^{Rts1}$ has an extensive role in regulating gene expression that will be explored in future studies.

The synthetic lethality observed between loss of Gcn5 and $PP2A^{Rts1}$ underscores our conclusion that the coordinate or parallel functions of these enzymes are fundamental for optimal growth and response to cell and genotoxic stress. Therefore, it is likely that there are multiple mechanisms of suppression by *RTS1* depending on type of stress, stage of the cell cycle, and other aspects of physiology. It is noteworthy that human Gcn5 is mutated or amplified in diverse cancers (Farria *et al.* 2015) and that the human B56 homolog of Rts1 has tumor suppressor function, although the mechanism(s) is incompletely understood (Li *et al.* 2007; Eichhorn *et al.* 2009).

Acknowledgments

We thank J. Hirsch and S. Roeder for the high-copy 2μ-plasmid library and A. Shilatifard for the SHIMA histone mutant plasmid library; A. Amon and D. Stillman for strains; R. Deshaies for the gift of the PP-B antibody; N. Mahajan for discussion; and these current and past L.P. lab members for critical feedback throughout the project and during preparation of the manuscript: Moriah Eustice, Bessie Xu, Ana Lilia Torres-Machorro, Renee Garza, Naomi Searle, Masha Evpak, Michael Hayes, and Jeremy Chen. We also thank the S. Berger lab for additional plasmids. E.L.P. is supported by American Cancer Society postdoctoral fellowship PF-13-283-01 and a Frontiers of Innovation Scholars Program award from the University of California, San Diego (UCSD). A.L. was supported by a Marie Curie outgoing international fellowship,

MOIFO40895. S.L.T. was an Amgen Scholar and the recipient of a Rae K. Hepps fellowship (UCSD). Support for this project was initiated with National Institutes of Health grants GM-56469 and GM-90177 and completed with support from the University of California's Cancer Research Coordinating Committee.

Literature Cited

Ahn, S. H., W. L. Cheung, J. Y. Hsu, R. L. Diaz, M. M. Smith *et al.*, 2005a Sterile 20 kinase phosphorylates histone H2B at serine 10 during hydrogen peroxide-induced apoptosis in *S. cerevisiae*. Cell 120: 25–36.

Ahn, S. H., K. A. Henderson, S. Keeney, and C. D. Allis, 2005b H2B (Ser10) phosphorylation is induced during apoptosis and meiosis in *S. cerevisiae*. Cell Cycle 4: 780–783.

Amberg, D. C., D. Burke, and J. N. Strathern, 2005 *Methods in Yeast Genetics: A Cold Spring Harbor Laboratory Course Manual*. Cold Spring Harbor Laboratory Press, Cold Spring Harbor, NY.

Amberg, D. C., D. J. Burke, and J. N. Strathern, 2006 Inducing yeast cell synchrony: α-factor arrest using *bar1* mutants. Cold Spring Harb Protoc.1. DOI: 10.1101/pdb.prot4173.

Artiles, K., S. Anastasia, D. McCusker, and D. R. Kellogg, 2009 The Rts1 regulatory subunit of protein phosphatase 2A is required for control of G1 cyclin transcription and nutrient modulation of cell size. PLoS Genet. 5: e1000727.

Azzam, R., S. L. Chen, W. Shou, A. S. Mah, G. Alexandru *et al.*, 2004 Phosphorylation by cyclin B-Cdk underlies release of mitotic exit activator Cdc14 from the nucleolus. Science 305: 516–519.

Baker, S. P., J. Phillips, S. Anderson, Q. Qiu, J. Shabanowitz *et al.*, 2010 Histone H3 Thr 45 phosphorylation is a replication-associated post-translational modification in *S. cerevisiae*. Nat. Cell Biol. 12: 294–298.

Banerjee, T., and D. Chakravarti, 2011 A peek into the complex realm of histone phosphorylation. Mol. Cell. Biol. 31: 4858–4873.

Bennett, G., and C. L. Peterson, 2015 SWI/SNF recruitment to a DNA double-strand break by the NuA4 and Gcn5 histone acetyltransferases. DNA Repair (Amst.) 30: 38–45.

Bialojan, C., and A. Takai, 1988 Inhibitory effect of a marine-sponge toxin, okadaic acid, on protein phosphatases. Specificity and kinetics. Biochem. J. 256: 283–290.

Bizzari, F., and A. L. Marston, 2011 Cdc55 coordinates spindle assembly and chromosome disjunction during meiosis. J. Cell Biol. 193: 1213–1228.

Burgess, R. J., H. Zhou, J. Han, and Z. Zhang, 2010 A role for Gcn5 in replication-coupled nucleosome assembly. Mol. Cell 37: 469–480.

Cayla, X., J. Goris, J. Hermann, P. Hendrix, R. Ozon *et al.*, 1990 Isolation and characterization of a tyrosyl phosphatase activator from rabbit skeletal muscle and *Xenopus laevis* oocytes. Biochemistry 29: 658–667.

Chan, L. Y., and A. Amon, 2009 The protein phosphatase 2A functions in the spindle position checkpoint by regulating the checkpoint kinase Kin4. Genes Dev. 23: 1639–1649.

Chang, J. S., and F. Winston, 2013 Cell-cycle perturbations suppress the slow-growth defect of spt10Delta mutants in *Saccharomyces cerevisiae*. G3 (Bethesda) 3: 573–583.

Cherry, J. M., E. L. Hong, C. Amundsen, R. Balakrishnan, G. Binkley *et al.*, 2012 Saccharomyces Genome Database: the genomics resource of budding yeast. Nucleic Acids Res. 40: D700–D705.

Cheung, P., K. G. Tanner, W. L. Cheung, P. Sassone-Corsi, J. M. Denu *et al.*, 2000 Synergistic coupling of histone H3 phosphorylation and acetylation in response to epidermal growth factor stimulation. Mol. Cell 5: 905–915.

Cho, U. S., and W. Xu, 2007 Crystal structure of a protein phosphatase 2A heterotrimeric holoenzyme. Nature 445: 53–7.

Clarke, A. S., J. E. Lowell, S. J. Jacobson, and L. Pillus, 1999 Esa1p is an essential histone acetyltransferase required for cell cycle progression. Mol. Cell. Biol. 19: 2515–2526.

Clayton, A. L., and L. C. Mahadevan, 2003 MAP kinase-mediated phosphoacetylation of histone H3 and inducible gene regulation. FEBS Lett. 546: 51–58.

Collins, S. R., K. M. Miller, N. L. Maas, A. Roguev, J. Fillingham *et al.*, 2007 Functional dissection of protein complexes involved in yeast chromosome biology using a genetic interaction map. Nature 446: 806–810.

Cosma, M. P., T. Tanaka, and K. Nasmyth, 1999 Ordered recruitment of transcription and chromatin remodeling factors to a cell cycle- and developmentally regulated promoter. Cell 97: 299–311.

Dimmer, K. S., S. Fritz, F. Fuchs, M. Messerschmitt, N. Weinbach *et al.*, 2002 Genetic basis of mitochondrial function and morphology in *Saccharomyces cerevisiae*. Mol. Biol. Cell 13: 847–853.

Downey, M., J. R. Johnson, N. E. Davey, B. W. Newton, T. L. Johnson *et al.*, 2015 Acetylome profiling reveals overlap in the regulation of diverse processes by sirtuins, Gcn5, and Esa1. Mol. Cell. Proteomics 14: 162–176.

Eberharter, A., D. E. Sterner, D. Schieltz, A. Hassan, J. R. Yates, 3rd *et al.*, 1999 The ADA complex is a distinct histone acetyltransferase complex in *Saccharomyces cerevisiae*. Mol. Cell. Biol. 19: 6621–6631.

Edmondson, D. G., J. K. Davie, J. Zhou, B. Mirnikjoo, K. Tatchell *et al.*, 2002 Site-specific loss of acetylation upon phosphorylation of histone H3. J. Biol. Chem. 277: 29496–29502.

Eichhorn, P. J., M. P. Creyghton, and R. Bernards, 2009 Protein phosphatase 2A regulatory subunits and cancer. Biochim. Biophys. Acta 1795: 1–15.

Eisenmann, D. M., C. Chapon, S. M. Roberts, C. Dollard, and F. Winston, 1994 The Saccharomyces cerevisiae SPT8 gene encodes a very acidic protein that is functionally related to SPT3 and TATA-binding protein. Genetics 137: 647–657.

Engebrecht, J., J. Hirsch, and G. S. Roeder, 1990 Meiotic gene conversion and crossing over: their relationship to each other and to chromosome synapsis and segregation. Cell 62: 927–937.

Eriksson, P. R., D. Ganguli, V. Nagarajavel, and D. J. Clark, 2012 Regulation of histone gene expression in budding yeast. Genetics 191: 7–20.

Farria, A., W. Li, and S. Y. Dent, 2015 KATs in cancer: functions and therapies. Oncogene 34: 4901–4913.

Fernius, J., and K. G. Hardwick, 2007 Bub1 kinase targets Sgo1 to ensure efficient chromosome biorientation in budding yeast mitosis. PLoS Genet. 3: e213.

Gentry, M. S., and R. L. Hallberg, 2002 Localization of *Saccharomyces cerevisiae* protein phosphatase 2A subunits throughout mitotic cell cycle. Mol. Biol. Cell 13: 3477–3492.

Ghule, P. N., R. L. Xie, R. Medina, J. L. Colby, S. N. Jones *et al.*, 2014 Fidelity of histone gene regulation is obligatory for genome replication and stability. Mol. Cell. Biol. 34: 2650–2659.

Grant, P. A., L. Duggan, J. Cote, S. M. Roberts, J. E. Brownell *et al.*, 1997 Yeast Gcn5 functions in two multisubunit complexes to acetylate nucleosomal histones: characterization of an Ada complex and the SAGA (Spt/Ada) complex. Genes Dev. 11: 1640–1650.

Grant, P. A., A. Eberharter, S. John, R. G. Cook, B. M. Turner *et al.*, 1999 Expanded lysine acetylation specificity of Gcn5 in native complexes. J. Biol. Chem. 274: 5895–5900.

Gunjan, A., and A. Verreault, 2003 A Rad53 kinase-dependent surveillance mechanism that regulates histone protein levels in *S. cerevisiae*. Cell 115: 537–549.

Guo, R., J. Chen, D. L. Mitchell, and D. G. Johnson, 2011 GCN5 and E2F1 stimulate nucleotide excision repair by promoting H3K9 acetylation at sites of damage. Nucleic Acids Res. 39: 1390–1397.

Guthrie, C., and G. R. Fink, 1991 *Guide to Yeast Genetics and Molecular Biology*. Academic Press, San Diego.

Haase, S. B., and S. I. Reed, 2002 Improved flow cytometric analysis of the budding yeast cell cycle. Cell Cycle 1: 132–136.

Haystead, T. A., A. T. Sim, D. Carling, R. C. Honnor, Y. Tsukitani *et al.*, 1989 Effects of the tumour promoter okadaic acid on intracellular protein phosphorylation and metabolism. Nature 337: 78–81.

Henry, K. W., A. Wyce, W. S. Lo, L. J. Duggan, N. C. Emre *et al.*, 2003 Transcriptional activation via sequential histone H2B ubiquitylation and deubiquitylation, mediated by SAGA-associated Ubp8. Genes Dev. 17: 2648–2663.

Howe, L., D. Auston, P. Grant, S. John, R. G. Cook *et al.*, 2001 Histone H3 specific acetyltransferases are essential for cell cycle progression. Genes Dev. 15: 3144–3154.

Huisinga, K. L., and B. F. Pugh, 2004 A genome-wide housekeeping role for TFIID and a highly regulated stress-related role for SAGA in *Saccharomyces cerevisiae*. Mol. Cell 13: 573–585.

Jiang, Y., 2006 Regulation of the cell cycle by protein phosphatase 2A in *Saccharomyces cerevisiae*. Microbiol. Mol. Biol. Rev. 70: 440–449.

Johansen, K. M., and J. Johansen, 2006 Regulation of chromatin structure by histone H3S10 phosphorylation. Chromosome Res. 14: 393–404.

Jonasson, E. M., V. Rossio, R. Hatakeyama, M. Abe, Y. Ohya *et al.*, 2016 Zds1/Zds2–PP2ACdc55 complex specifies signaling output from Rho1 GTPase. J. Cell Biol. 212: 51–61.

Kennedy, E. K., M. Dysart, N. Lianga, E. C. Williams, S. Pilon *et al.*, 2016 Redundant regulation of Cdk1 tyrosine dephosphorylation in *Saccharomyces cerevisiae*. Genetics 202: 903–910.

Krebs, J. E., M. H. Kuo, C. D. Allis, and C. L. Peterson, 1999 Cell cycle-regulated histone acetylation required for expression of the yeast HO gene. Genes Dev. 13: 1412–1421.

Lafon, A., E. Petty, and L. Pillus, 2012 Functional antagonism between Sas3 and Gcn5 acetyltransferases and ISWI chromatin remodelers. PLoS Genet. 8: 1002994.

Lee, H. S., J. H. Park, S. J. Kim, S. J. Kwon, and J. Kwon, 2010 A cooperative activation loop among SWI/SNF, gamma-H2AX and H3 acetylation for DNA double-strand break repair. EMBO J. 29: 1434–1445.

Lee, K. K., M. E. Sardiu, S. K. Swanson, J. M. Gilmore, M. Torok *et al.*, 2011 Combinatorial depletion analysis to assemble the network architecture of the SAGA and ADA chromatin remodeling complexes. Mol. Syst. Biol. 7: 503.

Li, H. H., X. Cai, G. P. Shouse, L. G. Piluso, and X. Liu, 2007 A specific PP2A regulatory subunit, B56gamma, mediates DNA damage-induced dephosphorylation of p53 at Thr55. EMBO J. 26: 402–411.

Liang, D., S. L. Burkhart, R. K. Singh, M. H. Kabbaj, and A. Gunjan, 2012 Histone dosage regulates DNA damage sensitivity in a checkpoint-independent manner by the homologous recombination pathway. Nucleic Acids Res. 40: 9604–9620.

Lo, W. S., R. C. Trievel, J. R. Rojas, L. Duggan, J. Y. Hsu *et al.*, 2000 Phosphorylation of serine 10 in histone H3 is functionally linked in vitro and in vivo to Gcn5-mediated acetylation at lysine 14. Mol. Cell 5: 917–926.

Magtanong, L., C. H. Ho, S. L. Barker, W. Jiao, A. Baryshnikova *et al.*, 2011 Dosage suppression genetic interaction networks enhance functional wiring diagrams of the cell. Nat. Biotechnol. 29: 505–511.

Mahajan, K., and N. P. Mahajan, 2013 WEE1 tyrosine kinase, a novel epigenetic modifier. Trends Genet. 29: 394–402.

Mahajan, K., B. Fang, J. M. Koomen, and N. P. Mahajan, 2012 H2B Tyr37 phosphorylation suppresses expression of replication-dependent core histone genes. Nat. Struct. Mol. Biol. 19: 930–937.

Meeks-Wagner, D., and L. H. Hartwell, 1986 Normal stoichiometry of histone dimer sets is necessary for high fidelity of mitotic chromosome transmission. Cell 44: 43–52.

Moore, J. D., O. Yazgan, Y. Ataian, and J. E. Krebs, 2007 Diverse roles for histone H2A modifications in DNA damage response pathways in yeast. Genetics 176: 15–25.

Nagy, Z., and L. Tora, 2007 Distinct GCN5/PCAF-containing complexes function as co-activators and are involved in transcription factor and global histone acetylation. Oncogene 26: 5341–5357.

Nakanishi, S., B. W. Sanderson, K. M. Delventhal, W. D. Bradford, K. Staehling-Hampton *et al.*, 2008 A comprehensive library of histone mutants identifies nucleosomal residues required for H3K4 methylation. Nat. Struct. Mol. Biol. 15: 881–888.

Nerusheva, O. O., S. Galander, J. Fernius, D. Kelly, and A. L. Marston, 2014 Tension-dependent removal of pericentromeric shugoshin is an indicator of sister chromosome biorientation. Genes Dev. 28: 1291–1309.

Parnell, E. J., Y. Yu, R. Lucena, Y. Yoon, L. Bai *et al.*, 2014 The Rts1 regulatory subunit of PP2A phosphatase controls expression of the HO endonuclease via localization of the Ace2 transcription factor. J. Biol. Chem. 289: 35431–35437.

Peplowska, K., A. U. Wallek, and Z. Storchova, 2014 Sgo1 regulates both condensin and Ipl1/Aurora B to promote chromosome biorientation. PLoS Genet. 10: e1004411.

Petty, E., and L. Pillus, 2013 Balancing chromatin remodeling and histone modifications in transcription. Trends Genet. 29: 621–629.

Pokholok, D. K., C. T. Harbison, S. Levine, M. Cole, N. M. Hannett *et al.*, 2005 Genome-wide map of nucleosome acetylation and methylation in yeast. Cell 122: 517–527.

Pollard, K. J., and C. L. Peterson, 1997 Role for ADA/GCN5 products in antagonizing chromatin-mediated transcriptional repression. Mol. Cell. Biol. 17: 6212–6222.

Pray-Grant, M. G., D. Schieltz, S. J. McMahon, J. M. Wood, E. L. Kennedy *et al.*, 2002 The novel SLIK histone acetyltransferase complex functions in the yeast retrograde response pathway. Mol. Cell. Biol. 22: 8774–8786.

Pray-Grant, M. G., J. A. Daniel, D. Schieltz, J. R. Yates, 3rd, and P. A. Grant, 2005 Chd1 chromodomain links histone H3 methylation with SAGA- and SLIK-dependent acetylation. Nature 433: 434–438.

Queralt, E., C. Lehane, B. Novak, and F. Uhlmann, 2006 Downregulation of PP2A(Cdc55) phosphatase by separase initiates mitotic exit in budding yeast. Cell 125: 719–732.

Rine, J., 1991 Gene overexpression in studies of *Saccharomyces cerevisiae*. Methods Enzymol. 194: 239–251.

Roberts, S. M., and F. Winston, 1996 SPT20/ADA5 encodes a novel protein functionally related to the TATA-binding protein and important for transcription in Saccharomyces cerevisiae. Mol. Cell. Biol. 16: 3206–3213.

Rosaleny, L. E., A. B. Ruiz-Garcia, J. Garcia-Martinez, J. E. Perez-Ortin, and V. Tordera, 2007 The Sas3p and Gcn5p histone acetyltransferases are recruited to similar genes. Genome Biol. 8(6): R119.

Rose, M. D., F. M. Winston, and P. Hieter, 1990 *Methods in Yeast Genetics: A Laboratory Course Manual*, Cold Spring Harbor Laboratory Press, Cold Spring Harbor, NY.

Rossetto, D., N. Avvakumov, and J. Cote, 2012 Histone phosphorylation: a chromatin modification involved in diverse nuclear events. Epigenetics 7: 1098–1108.

Rossio, V., and S. Yoshida, 2011 Spatial regulation of Cdc55–PP2A by Zds1/Zds2 controls mitotic entry and mitotic exit in budding yeast. J. Cell Biol. 193: 445–454.

Ruault, M., and L. Pillus, 2006 Chromatin-modifiying enzymes are essential when the *Saccharomyces cerevisiae* morphogenesis checkpoint is constitutively activated. Genetics 174: 1135–1149.

Sasaki, K., M. Murata, T. Yasumoto, G. Mieskes, and A. Takai, 1994 Affinity of okadaic acid to type-1 and type-2A protein phosphatases is markedly reduced by oxidation of its 27-hydroxyl group. Biochem. J. 298(Pt 2): 259–262.

Sawicka, A., and C. Seiser, 2014 Sensing core histone phosphorylation: a matter of perfect timing. Biochim. Biophys. Acta 1839: 711–718.

Sawicka, A., D. Hartl, M. Goiser, O. Pusch, R. R. Stocsits *et al.*, 2014 H3S28 phosphorylation is a hallmark of the transcriptional response to cellular stress. Genome Res. 24: 1808–1820.

Schneider, C. A., W. S. Rasband, and K. W. Eliceiri, 2012 NIH Image to ImageJ: 25 years of image analysis. Nat. Methods 9: 671–675.

Seshacharyulu, P., P. Pandey, K. Datta, and S. K. Batra, 2013 Phosphatase: PP2A structural importance, regulation and its aberrant expression in cancer. Cancer Lett. 335: 9–18.

Singh, R. K., M. H. Kabbaj, J. Paik, and A. Gunjan, 2009 Histone levels are regulated by phosphorylation and ubiquitylation-dependent proteolysis. Nat. Cell Biol. 11: 925–933.

Singh, R. K., D. Liang, U. R. Gajjalaiahvari, M. H. Kabbaj, J. Paik *et al.*, 2010 Excess histone levels mediate cytotoxicity via multiple mechanisms. Cell Cycle 9: 4236–4244.

Sontag, J. M., and E. Sontag, 2014 Protein phosphatase 2A dysfunction in Alzheimer's disease. Front. Mol. Neurosci. 7: 16.

Sterner, D. E., P. A. Grant, S. M. Roberts, L. J. Duggan, R. Belotserkovskaya *et al.*, 1999 Functional organization of the yeast SAGA complex: distinct components involved in structural integrity, nucleosome acetylation, and TATA-binding protein interaction. Mol. Cell. Biol. 19: 86–98.

Sterner, D. E., R. Belotserkovskaya, and S. L. Berger, 2002 SALSA, a variant of yeast SAGA, contains truncated Spt7, which correlates with activated transcription. Proc. Natl. Acad. Sci. USA 99: 11622–11627.

Sugiyama, M., and J. Nikawa, 2001 The *Saccharomyces cerevisiae* Isw2p-Itc1p complex represses *INO1* expression and maintains cell morphology. J. Bacteriol. 183: 4985–4993.

Sugiyama, M., S. P. Akase, R. Nakanishi, H. Horie, Y. Kaneko *et al.*, 2014 Nuclear localization of Haa1, which is linked to its phosphorylation status, mediates lactic acid tolerance in *Saccharomyces cerevisiae*. Appl. Environ. Microbiol. 80: 3488–3495.

Swingle, M., L. Ni, and R. E. Honkanen, 2007 Small-molecule inhibitors of ser/thr protein phosphatases: specificity, use and common forms of abuse. Methods Mol. Biol. 365: 23–38.

Tessarz, P., and T. Kouzarides, 2014 Histone core modifications regulating nucleosome structure and dynamics. Nat. Rev. Mol. Cell Biol. 15: 703–708.

Tkach, J. M., A. Yimit, A. Y. Lee, M. Riffle, M. Costanzo *et al.*, 2012 Dissecting DNA damage response pathways by analysing protein localization and abundance changes during DNA replication stress. Nat. Cell Biol. 14: 966–976.

Venters, B. J., S. Wachi, T. N. Mavrich, B. E. Andersen, P. Jena *et al.*, 2011 A comprehensive genomic binding map of gene and chromatin regulatory proteins in *Saccharomyces*. Mol. Cell 41: 480–492.

Vernarecci, S., P. Ornaghi, A. Bagu, E. Cundari, P. Ballario *et al.*, 2008 Gcn5p plays an important role in centromere kinetochore function in budding yeast. Mol. Cell. Biol. 28: 988–996.

Verzijlbergen, K. F., O. O. Nerusheva, D. Kelly, A. Kerr, D. Clift *et al.*, 2014 Shugoshin biases chromosomes for biorientation through condensin recruitment to the pericentromere. eLife 3: e01374.

Virshup, D. M., and S. Shenolikar, 2009 From promiscuity to precision: protein phosphatases get a makeover. Mol. Cell 33: 537–545.

Wang, L., L. Liu, and S. L. Berger, 1998 Critical residues for histone acetylation by Gcn5, functioning in Ada and SAGA complexes, are also required for transcriptional function in vivo. Genes Dev. 12: 640–653.

Wang, Y., and T. Y. Ng, 2006 Phosphatase 2A negatively regulates mitotic exit in *Saccharomyces cerevisiae*. Mol. Biol. Cell 17: 80–89.

Warfield, L., J. A. Ranish, and S. Hahn, 2004 Positive and negative functions of the SAGA complex mediated through interaction of Spt8 with TBP and the N-terminal domain of TFIIA. Genes Dev. 18: 1022–1034.

Wu, P. Y., C. Ruhlmann, F. Winston, and P. Schultz, 2004 Molecular architecture of the *S. cerevisiae* SAGA complex. Mol. Cell 15: 199–208.

Xue, Y., J. Ren, X. Gao, C. Jin, L. Wen *et al.*, 2008 GPS 2.0, a tool to predict kinase-specific phosphorylation sites in hierarchy. Mol. Cell. Proteomics 7: 1598–1608.

Yang, J., and C. Phiel, 2010 Functions of B56-containing PP2As in major developmental and cancer signaling pathways. Life Sci. 87: 659–666.

Yellman, C. M., and D. J. Burke, 2006 The role of Cdc55 in the spindle checkpoint is through regulation of mitotic exit in *Saccharomyces cerevisiae*. Mol. Biol. Cell 17: 658–666.

Zapata, J., N. Dephoure, T. Macdonough, Y. Yu, E. J. Parnell *et al.*, 2014 PP2ARts1 is a master regulator of pathways that control cell size. J. Cell Biol. 204: 359–376.

Zentner, G. E., T. Tsukiyama, and S. Henikoff, 2013 ISWI and CHD chromatin remodelers bind promoters but act in gene bodies. PLoS Genet. 9: e1003317.

Zhang, W., J. R. Bone, D. G. Edmondson, B. M. Turner, and S. Y. Roth, 1998 Essential and redundant functions of histone acetylation revealed by mutation of target lysines and loss of the Gcn5p acetyltransferase. EMBO J. 17: 3155–3167.

Communicating editor: M. Hampsey

GENETICS

Supporting Information
www.genetics.org/lookup/suppl/doi:10.1534/genetics.116.189506/-/DC1

Promotion of Cell Viability and Histone Gene Expression by the Acetyltransferase Gcn5 and the Protein Phosphatase PP2A in *Saccharomyces cerevisiae*

Emily L. Petty, Anne Lafon, Shannon L. Tomlinson, Bryce A. Mendelsohn, and Lorraine Pillus

DOI: 10.1534/genetics.116.189506

Figure S1.

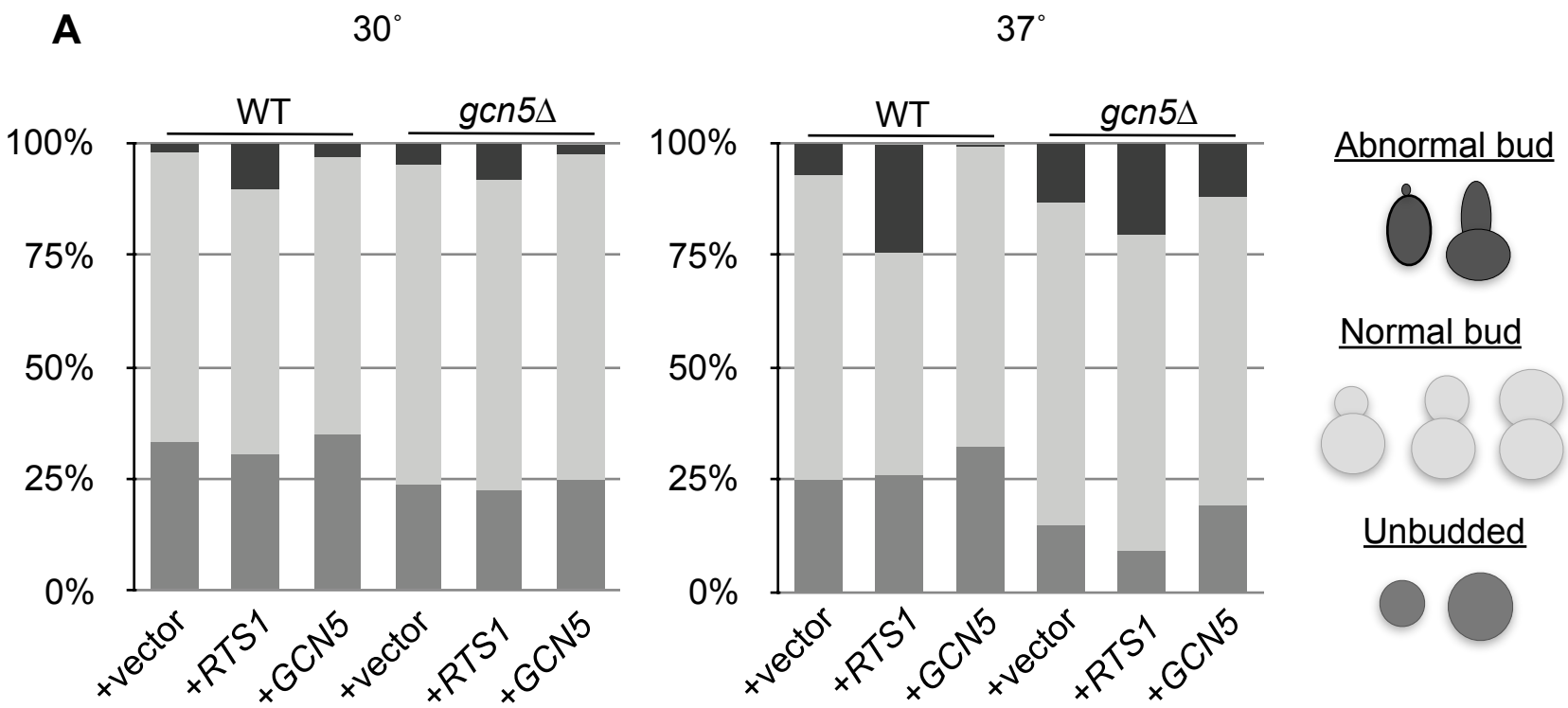

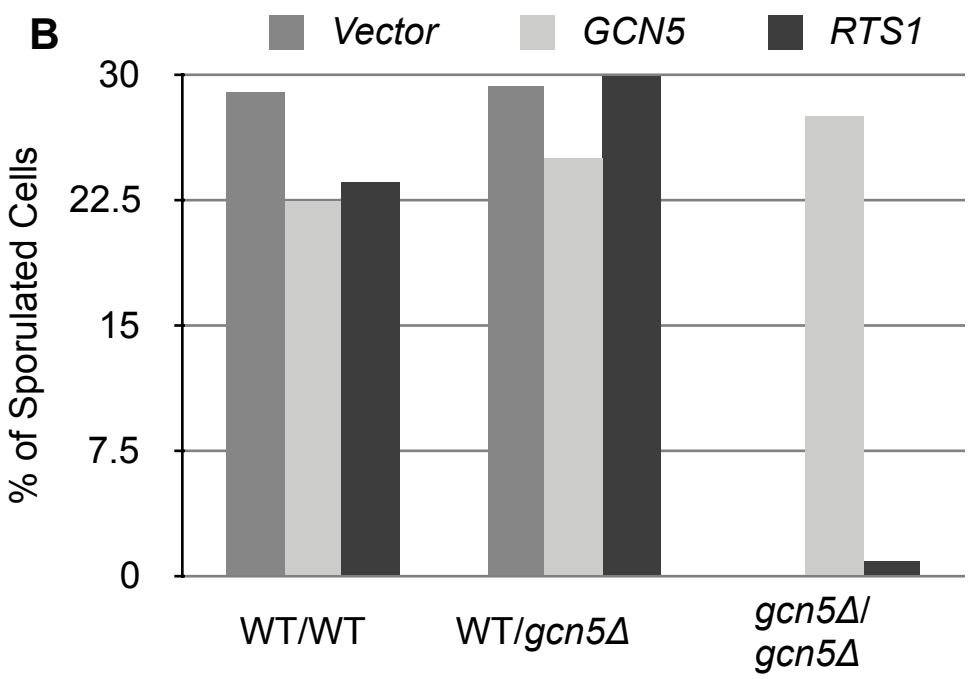

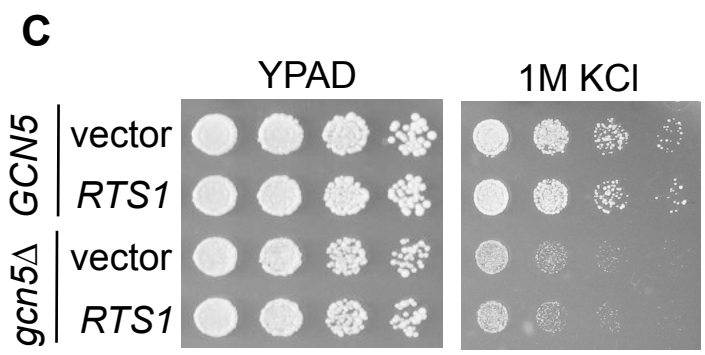

D

*gcn5*Δ phenotype	Suppression by *RTS1* overexpression
Temperature sensitivity	+
DNA damage sensitivity	+
Bud morphology defect	-
Sporulation defect	-
Cell cycle progression defect	+
Osmotic defect	-
Poor growth on non-fermentable carbon sources	+

Figure S2.

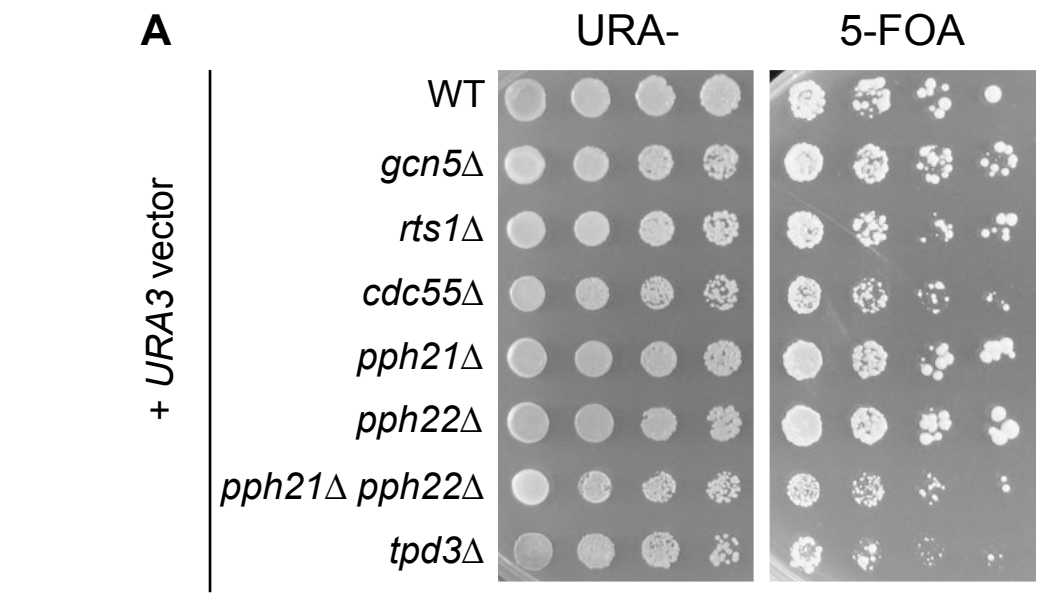
A
URA-
5-FOA
+ URA3 vector
WT
gcn5Δ
rts1Δ
cdc55Δ
pph21Δ
pph22Δ
pph21Δ pph22Δ
tpd3Δ
B
30˚
36˚
37˚
WT
gcn5Δ
gcn5Δ cdc55Δ
C
Cdc55
Pph21/22
Tpd3
PP2A^Cdc55
WT+vec
WT+RTS1
gcn5Δ+vec
gcn5Δ+RTS1
cdc55Δ+vec
Net1ph
Tubulin
37˚

Figure S3.

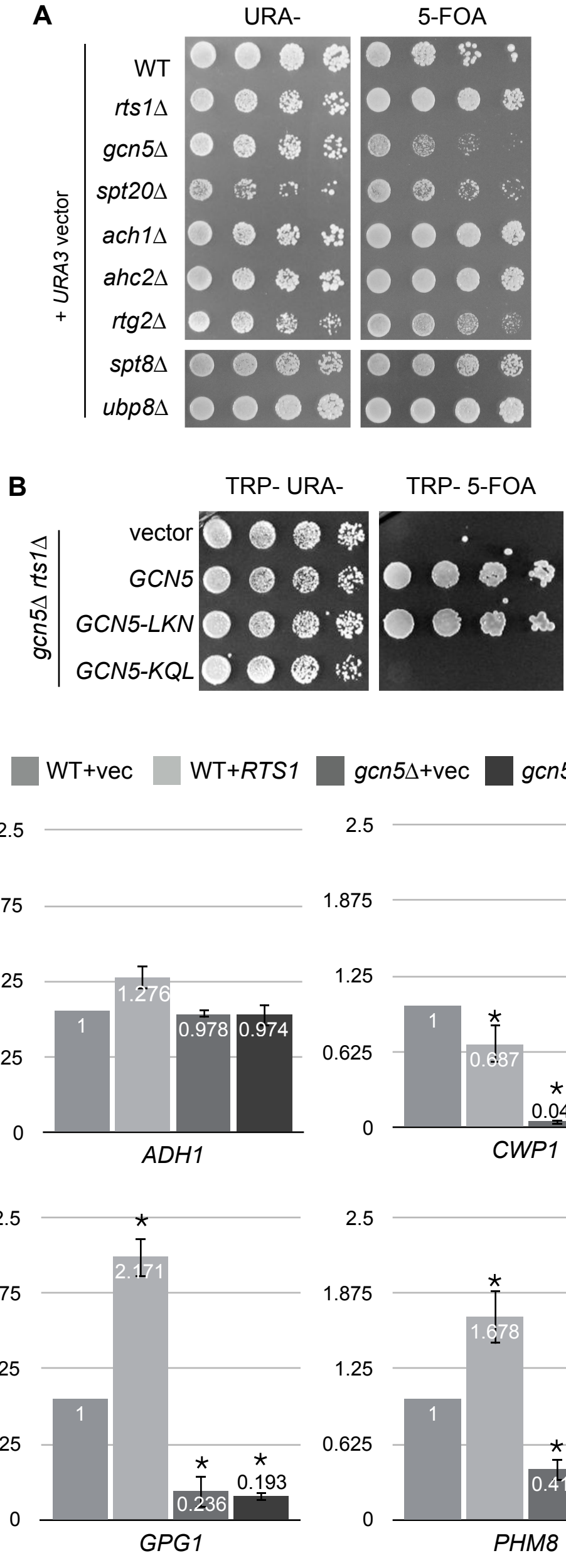
A
URA-
5-FOA
+ URA3 vector
WT
rts1Δ
gcn5Δ
spt20Δ
ach1Δ
ahc2Δ
rtg2Δ
spt8Δ
ubp8Δ
B
TRP- URA-
TRP- 5-FOA
gcn5Δ rts1Δ
vector
GCN5
GCN5-LKN
GCN5-KQL
C
WT+vec
WT+RTS1
gcn5Δ+vec
gcn5Δ+RTS1
relative mRNA levels
2.5
1.875
1.25
0.625
0
ADH1
1
1.276
0.978
0.974
CWP1
0.687
0.042
0.023
GPG1
2.171
0.236
0.193
PHM8
1.678
0.414
0.223
*

Figure S4.

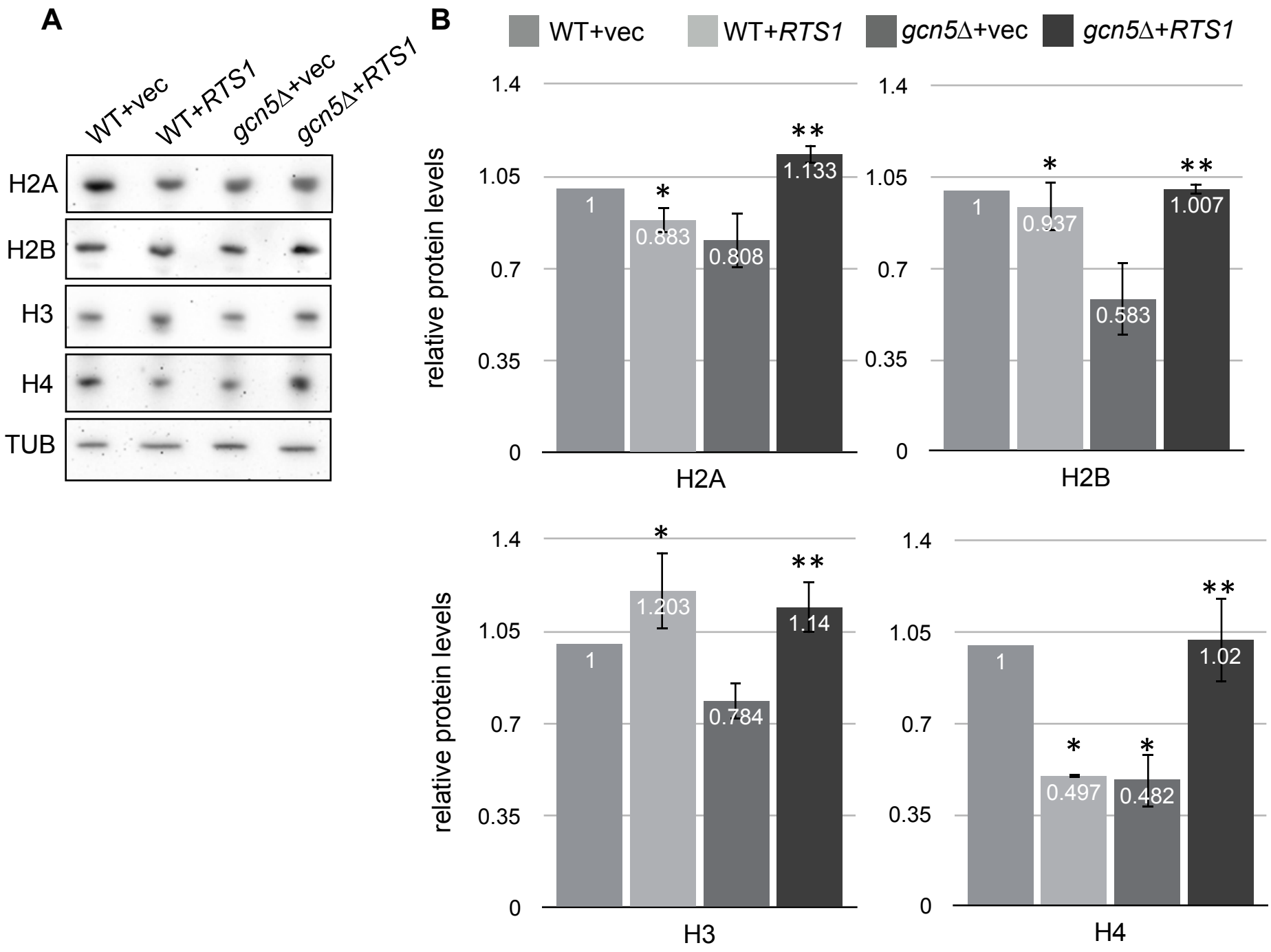
A
WT+vec
WT+RTS1
gcn5Δ+vec
gcn5Δ+RTS1
H2A
H2B
H3
H4
TUB
B
WT+vec
WT+RTS1
gcn5Δ+vec
gcn5Δ+RTS1
relative protein levels
1.4
1.05
0.7
0.35
0
1
0.883
0.808
1.133
H2A
1
0.937
0.583
1.007
H2B
1
1.203
0.784
1.14
H3
1
0.497
0.482
1.02
H4
*
**

Figure S5.

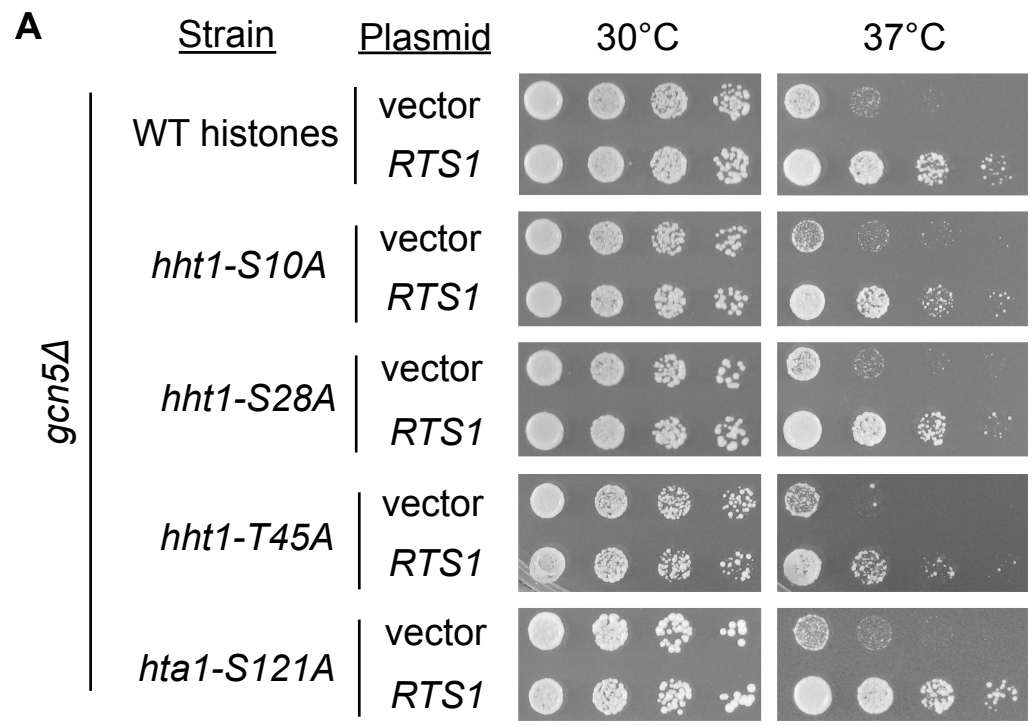
A
Strain
Plasmid
30°C
37°C
gcn5Δ
WT histones
vector
RTS1
hht1-S10A
vector
RTS1
hht1-S28A
vector
RTS1
hht1-T45A
vector
RTS1
hta1-S121A
vector
RTS1

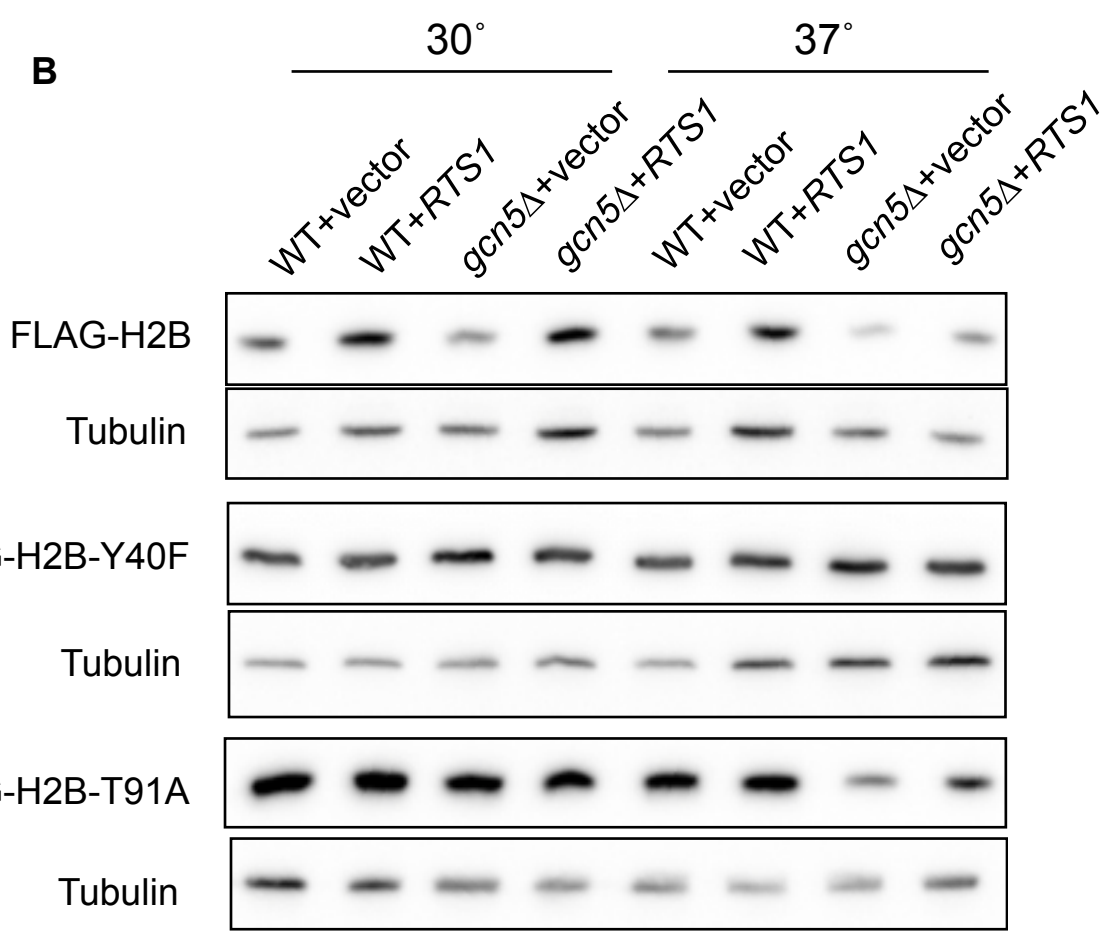
B
30˚
37˚
WT+vector
WT+RTS1
gcn5Δ+vector
gcn5Δ+RTS1
WT+vector
WT+RTS1
gcn5Δ+vector
gcn5Δ+RTS1
FLAG-H2B
Tubulin
FLAG-H2B-Y40F
Tubulin
FLAG-H2B-T91A
Tubulin

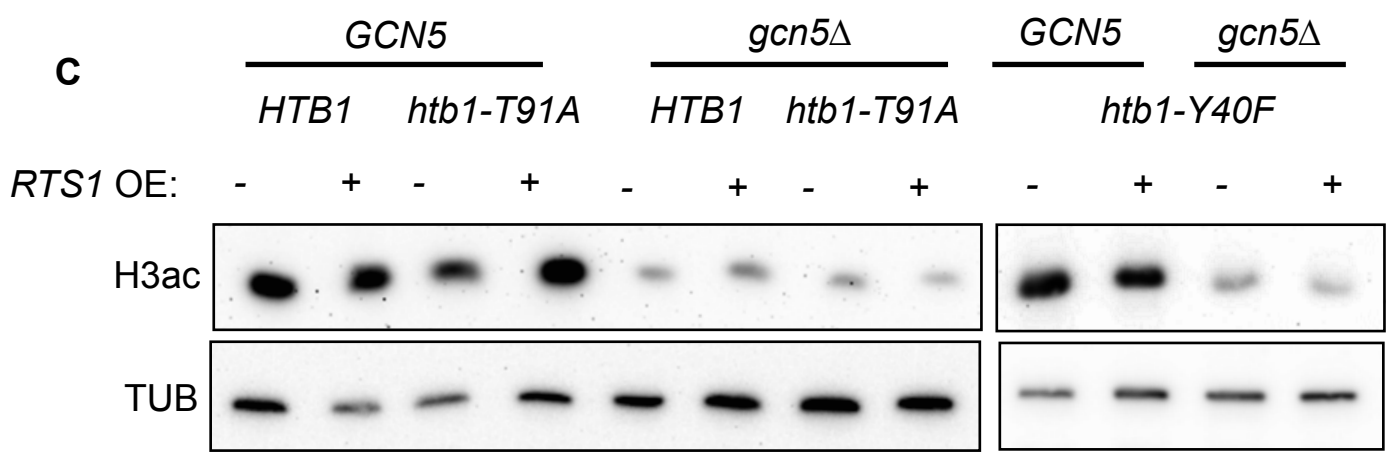
C
GCN5
gcn5Δ
GCN5
gcn5Δ
HTB1
htb1-T91A
HTB1
htb1-T91A
htb1-Y40F
RTS1 OE:
- + - + - + - + - + - +
H3ac
TUB

Figure S6.

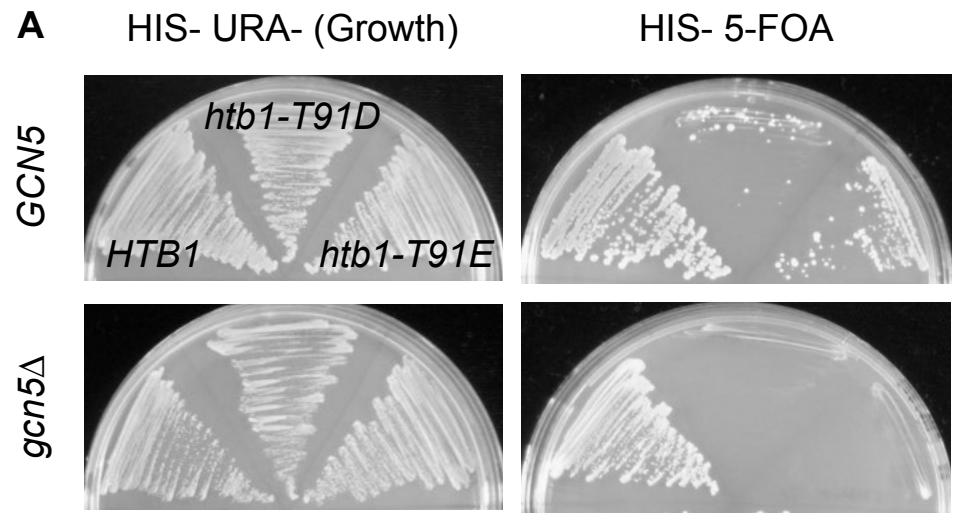
A
HIS- URA- (Growth)
HIS- 5-FOA
GCN5
gcn5Δ
htb1-T91D
HTB1
htb1-T91E

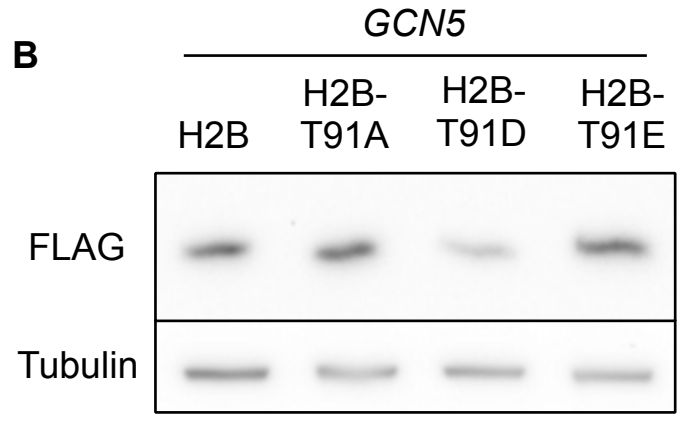
B
GCN5
H2B
H2B-T91A
H2B-T91D
H2B-T91E
FLAG
Tubulin

Table S1. List of Strains

STRAIN	GENOTYPE
LPY5	MATa *ade2-1 can1-100 his3-11 leu2-3,112 trp1-1 ura3-1 GAL*
LPY1552	MATa/MATα *ade2-1/ade2-1 can1-100/can1-100 his3-11/his3-11 leu2-3,112/leu2-3,112 trp1-1/trp1-1 ura3-1ura3-1 GAL/GAL*
LPY6487	MATa *ade2-1 can1-100 his3-11 leu2-3,112 trp1-1 ura3-1 GAL spt8Δ::kanMX*
LPY8240	MATa *ade2-1 can1-100 his3-11 leu2-3,112 trp1-1 ura3-1 GAL ubp8Δ::kanMX*
LPY10182	MATa *ade2-1 can1-100 his3-11 leu2-3,112 trp1-1 ura3-1 GAL gcn5Δ::kanMX*
LPY11437	MATα *ade2-1 can1-100 his3-11 leu2-3,112 trp1-1 ura3-1 GAL gcn5Δ::kanMX sasΔ::HIS3 ura3::C357Y, P375A – URA3*
LPY11975	MATa *ade2-1 can1-100 his3-11 leu2-3,112 trp1-1 ura3-1 GAL bar1Δ::kanMX*
LPY12231	MATα *ade2-1 can1-100 his3-11 leu2-3,112 trp1-1 ura3-1 GAL hht1- hhf1Δ::kanMX hht2-hhf2Δ::kanMX hta2-htb2Δ::HPH* + pLP2212
LPY13321	MATα *ade2-1 can1-100 his3-11 leu2-3,112 trp1-1 GAL gcn5Δ::NatMX sas3Δ::HIS ura3-1::sas3 C357Y, P375A-URA3*
LPY13435	MATa *ade2-1 can1-100 his3-11 leu2-3,112 trp1-1 ura3-1 GAL gcn5Δ::NatMX*
LPY13846	MATα *ade2-1 can1-100 his3-11 leu2-3,112 trp1-1 ura3-1 GAL gcn5Δ::kanMX snf1Δ::TRP1*
LPY14461	MATα *ade2-1 can1-100 his3-11 leu2-3,112 trp1-1 ura3-1 GAL hht1- hhf1Δ::kanMX hta1-htb1Δ::natMX hta2-htb2Δ::HPH* + pLP2212
LPY14642	MATa *ade2-1 can1-100 his3-11 leu2-3,112 trp1-1 ura3-1 GAL pph21Δ::kanMX*
LPY14644	MATa *ade2-1 can1-100 his3-11 leu2-3,112 trp1-1 ura3-1 GAL gcn5Δ::kanMX pph21Δ::kanMX*

Table S1. List of Strains

STRAIN	GENOTYPE
LPY14653	MATa *ade2-1 can1-100 his3-11 leu2-3,112 trp1-1 ura3-1 GAL rts1Δ::kanMX*
LPY14690	MATa *ade2-1 can1-100 his3-11 leu2-3,112 trp1-1 ura3-1 GAL pph22Δ::kanMX*
LPY14692	MATa *ade2-1 can1-100 his3-11 leu2-3,112 trp1-1 ura3-1 GAL gcn5Δ::kanMX pph22Δ::kanMX*
LPY15178	MATa *ade2-1 can1-100 his3-11 leu2-3,112 trp1-1 ura3-1 GAL gcn5Δ::natMX rts1Δ::kanMX* + pLP1640
LPY15180	MATa/MATα *ade2-1/ade2-1 can1-100/can1-100 his3-11/his3-11 leu2-3,112/leu2-3,112 trp1-1/trp1-1 ura3-1ura3-1 GAL/GAL gcn5Δ::natMX/gcn5Δ::natMX*
LPY15267	MATa *ade2-1 can1-100 his3-11 leu2-3,112 trp1-1 ura3-1 GAL pph21Δ::KanMX pph21Δ::KanMX*
LPY15296	MATa *ade2-1 can1-100 his3-11 leu2-3,112 ura3-1 GAL cdc55Δ::kanMX6 gcn5Δ::natMX*+pLP1640
LPY15297	MATα *ade2-1 can1-100 his3-11 leu2-3,112 ura3-1 GAL cdc55Δ::kanMX6* +pLP1640
LPY15328	MATa/MATα *ade2-1/ade2-1 can1-100/can1-100 his3-11/his3-11 leu2-3,112/leu2-3,112 trp1-1/trp1-1 ura3-1ura3-1 GAL/GAL gcn5Δ::natMX/GCN5 tpd3Δ::kanMX/TPD3*
LPY15416	MATa *ade2-1 can1-100 his3-11 leu2-3,112 trp1-1 ura3-1 GAL gcn5Δ::natMX tpd3Δ::kanMX* +pLP1640
LPY15417	MATa *ade2-1 can1-100 his3-11 leu2-3,112 trp1-1 ura3-1 GAL tpd3Δ::kanMX*
LPY15460	MATa/MATα *ade2-1/ade2-1 can1-100/can1-100 his3-11/his3-11 leu2-3,112/leu2-3,112 trp1-1/trp1-1 ura3-1ura3-1 GAL/GAL gcn5Δ::natMX/GCN5*
LPY16290	MATa *ade2-1 can1-100 his3-11 leu2-3,112 trp1-1 ura3-1 GAL hht1- hhf1Δ:kanMX hht2-hhf2Δ::kanMX hta2-htb2Δ::HPH gcn5Δ::kanMX* + pLP2212

Table S1. List of Strains

STRAIN	GENOTYPE
LPY16346	MATα *ade2-1 can1-100 his3-11 leu2-3,112 trp1-1 ura3-1 GAL hht1- hhf1Δ::kanMX hta1-htb1Δ::NAT hta2-htb2Δ::HPH rts1Δ::kanMX* + pLP2212
LPY16432	MATa *ade2-1 can1-100 his3-11 leu2-3,112 trp1-1 ura3-1 GAL hht1- hhf1Δ::kanMX hht2-hhf2Δ::kanMX hta2-htb2Δ::HPH sas3Δ::kanMX* + pLP2212
LPY16434	MATa *ade2-1 can1-100 his3-11 leu2-3,112 trp1-1 ura3-1 GAL hht1-hhf1Δ::kanMX hta1-htb1Δ::natMX hta2-htb2Δ::HPH gcn5Δ::kanMX* + pLP2212
LPY16456	MATa *ade2-1 can1-100 his3-11 leu2-3,112 trp1-1 ura3-1 GAL sch9Δ::kanMX*
*LPY16914	MATa *ade2-1 can1-100 his3-11 leu2-3,112 trp1-1 ura3-1 spt20Δ::HIS3*
LPY16980	MATα *ade2-1 can1-100 his3-11 leu2-3,112 trp1-1 ura3-1 GAL rts1Δ::kanMX*
LPY17138	MATa *ade2-1 can1-100 his3-11 leu2-3,112 trp1-1 ura3-1 GAL gcn5Δ::natMX sch9Δ::kanMX* + pLP1640
LPY17139	MATα *ade2-1 can1-100 his3-11 leu2-3,112 trp1-1 ura3-1 GAL gcn5Δ::natMX sch9Δ::kanMX*
LPY17140	MATa *ade2-1 can1-100 his3-11 leu2-3,112 trp1-1 ura3-1 GAL gcn5Δ::natMX sch9Δ::kanMX*
LPY17370	MATa *ade2-1 can1-100 his3-11 leu2-3,112 trp1-1 ura3-1 GAL ahc1Δ::kanMX*
LPY17484	MATa *ade2-1 can1-100 his3-11 leu2-3,112 trp1-1 ura3-1 GAL rts1Δ::kanMX spt20Δ::HIS3*
LPY18184	MATa *ade2-1 can1-100 his3-11 leu2-3,112 trp1-1 ura3-1 GAL rtg2Δ::kanMX*
LPY18424	MATa *ade2-1 can1-100 his3-11 leu2-3,112 trp1-1 ura3-1 GAL rts1Δ::kanMX ahc1Δ::kanMX* +pLP2462
LPY18518	MATa *ade2-1 can1-100 his3-11 leu2-3,112 trp1-1 ura3-1 GAL ahc2Δ::kanMX*
LPY18495	MATa *ade2-1 can1-100 his3-11 leu2-3,112 trp1-1 ura3-1 GAL rts1Δ::kanMX ahc2Δ::kanMX* +pLP2462

Table S1. List of Strains

STRAIN	GENOTYPE
LPY20692	MATa *ade2-1 can1-100 his3-11 leu2-3,112 trp1-1 ura3-1 GAL rts1*Δ*::kanMX rtg2*Δ*::kanMX*
LPY20694	MATa *ade2-1 can1-100 his3-11 leu2-3,112 trp1-1 ura3-1 GAL gcn5*Δ*::natMX pph21*Δ*::kanMX pph22*Δ*::kanMX* + pLP2997
LPY21081	MATa *ade2-1 can1-100 his3-11 leu2-3,112 trp1-1 ura3-1 GAL rts1*Δ*::kanMX ubp8*Δ*::kanMX* + pLP2462
LPY21272	MATa *ade2-1 can1-100 his3-11 leu2-3,112 trp1-1 ura3-1 GAL bar1*Δ*::kanMX gcn5*Δ*::natMX*
LPY21898	MATa *ade2-1 can1-100 his3-11 leu2-3,112 trp1-1 ura3-1 GAL rts1*Δ*::kanMX spt8*Δ*::kanMX* + pLP2462

Except where indicated (*), all strains are from the lab collection.

* LPY16914 is a gift of D. Stillman

Table S2. List of Plasmids

pLP NUMBER	GENE	MARKER/COPYNUMBER	SOURCE
61	Vector	*TRP1*/CEN	
126	Vector	*URA3*/CEN	
135	Vector	*LEU2*/2μ	
136	Vector	*URA3*/2μ	
645	*SAS3*	*LEU2*/2μ	
1518	*GCN5*	*TRP1*/CEN	
1520	*GCN5-LKN*	*TRP1*/*CEN*	Wang et al. (1998); S. Berger lab
1521	*GCN5-KQL*	*TRP1*/CEN	Wang et al. (1998); S. Berger lab
1524	*GCN5*	*LEU2*/2μ	
1640	*GCN5*	*URA3*/CEN	
1641	*GCN5*	*URA3*/2μ	
2131	*HTA1 HTB1*	*HIS3*/CEN	Ingvarsdottir et al., (2005); S. Berger lab
2197	*RTS1*	*LEU2*/2μ	
2212	*HTA1 HTB1 HHT2 HHF2*	*URA3*/CEN	
2330	*CDC55*	*LEU2*/2μ	
2433	*HHT2 HHF2*	*TRP1*/CEN	Nakanishi et al., (2008)

2436	*hht2-S10A HHF2*	*TRP1*/CEN	Nakanishi et al., (2008)
2439	*hht2-S28A HHF2*	*TRP1*/CEN	Nakanishi et al., (2008)
2462	*RTS1*	*URA3*/2μ	
2481	*HTA1 htb1-S90A-FLAG*	*HIS3*/CEN	Nakanishi et al., (2008)
2482	*HTA1 htb1-T91A-FLAG*	*HIS3*/CEN	Nakanishi et al., (2008)
2492	*HTA1 HTB1-FLAG*	*HIS3*/CEN	Nakanishi et al., (2008)
2501	*hta-S121A HTB-FLAG*	*HIS3*/CEN	Nakanishi et al., (2008)
2515	*hht2-T45A HHF2*	*TRP1*/CEN	Nakanishi et al., (2008)
2689	*HTA1 htb1-T91E-FLAG*	*HIS3/CEN*	Nakanishi et al., (2008); this study
2770	*HTA1 htb1-T91D-FLAG*	*HIS3*/CEN	Nakanishi et al., (2008); this study
2997	*PPH22*	*URA3*/CEN	
3250	*HTA1 htb1-Y40F-FLAG*	*HIS3*/CEN	Nakanishi et al., (2008); this study
3251	*HTA1 htb1-Y43F-FLAG*	*HIS3*/CEN	Nakanishi et al., (2008); this study

Except where indicated, plasmids listed were constructed in the Pillus lab.

Table S3. List of Primers

OLP NUMBER	GENE	USE	SEQUENCE
1275	*SCR1*	qPCR control	CGCGGCTAGACACGGATT
1276	*SCR1*	qPCR control	GCACGGTGCGGAATAGAGAA
1586	*SCH9*	Deletion	GCGCCAGTTCCCGCCTGC
1587	*SCH9*	Deletion	CGCGCATCGATGAGCCCTGCC
1643	*HTB1*	Mutagenesis	CGTATAACAAGAAGTCTGAGATCTCTGCTAGAG
1644	*HTB1*	Mutagenesis	CTCTAGCAGAGATCTCAGACTTCTTGTTATACG
1645	*HTB1*	Mutagenesis	GCTACTGAAGCTTCTGCATTGGCTGCGTATAAC
1646	*HTB1*	Mutagenesis	GTTATACGCAGCCAATGCAGAAGCTTCAGTAG
1647	*HTB1*	Mutagenesis	GGCTGCGTATAACGCGAAGTCTGCTATC
1648	*HTB1*	Mutagenesis	GATAGCAGACTTCGCGTTATACGCAGCC
1685	*HTB1*	Mutagenesis	CGTATAACAAGAAGTCTGCTATCTCTGCTAGAG
1686	*HTB1*	Mutagenesis	CTCTAGCAGAGATAGCAGACTTCTTGTTATACG
1754	*HTB1*	Mutagenesis	GCTGCGTATAACAAGAAGTCTGACATCTCTGCTAGAG
1755	*HTB1*	Mutagenesis	CTCTAGCAGAGATGTCAGACTTCTTGTTATACGCAGC
1789	*AHC1*	Deletion	GCCACTGTGCATAGCCG
1790	*AHC1*	Deletion	GGGTACGTCTATGGC

Table S3. List of Primers

2060	*HTA1*	qPCR	TGTCTTGGAATATTTGGCCG
2061	*HTA1*	qPCR	TGGATGTTTGGCAAAACACC
2064	*HTA2*	qPCR	GCTGTCTTAGAATATTTGGCTGC
2065	*HTA2*	qPCR	GGCAACAAGTTTTGGTGAATG
2058	*HTB1*	qPCR	GGTAAGAAGAGAAGCAAGGCTAGAA
2059	*HTB1*	qPCR	GACTTCTTGTTATACGCAGCCA
2062	*HTB2*	qPCR	GTCGATGGTAAGAAGAGATCTAAGG
2063	*HTB2*	qPCR	GTGGATTTCTTGTTATAAGCGGC
2070	*HHF1*	qPCR	TAAAGGTCTAGGTAAAGGTGGTGC
2071	*HHF1*	qPCR	TAACAGAGTCTCTGATGACGGATT
2066	*HHT1*	qPCR	GCTTTGAGAGAAATCAGAAGATTCC
2067	*HHT1*	qPCR	GCAGCCAAGTTGGTATCTTCAA
2068	*HHT2*	qPCR	CTGTTGCCTTGAGAGAAATTAGAAG
2069	*HHT2*	qPCR	GCAGCCAGATTAGTGTCTTCAAAC
2182	*HHF2*	qPCR	TAAAGGTCTAGGAAAAGGTGGTGC
2183	*HHF2*	qPCR	TAACAGAGTCCCTGATGACGGATT
2233	*ADH1*	qPCR	CGGTCACTGGGTTGCTATCT
2234	*ADH1*	qPCR	CCGTCAGTGGCCTTTAGAAC

Table S3. List of Primers

2229	*CWP*	qPCR	CTAGCTCCCCAACTGCTTCA
2230	*CWP*	qPCR	GGCACCTGCATTTTCTGTTT
2231	*GPG1*	qPCR	CAAAGATGGCAGTGTTGTGG
2232	*GPG1*	qPCR	GTCACCGTTGTCGGAGAGTT
2235	*PHM8*	qPCR	AAGGTGATTTGGAGGCAGAC
2236	*PHM8*	qPCR	AAGTGGCCTTGGGTTTTCTT

Table S4. Normalized averages and significant p-values for quantitative data			
Figure	Transformant	Normalized Average	p-value
3D	WT+vector (DMSO)	1	
3D	WT+vector (OKA)	1	
3D	WT+*RTS1* (DMSO)	0.823	
3D	WT+*RTS1* (OKA)	0.62	
3D	*gcn5*Δ+vector (DMSO)	0.42	
3D	*gcn5*Δ+vector (OKA)	0.36	
3D	*gcn5*Δ+*RTS1* (DMSO)	1.01	
3D	*gcn5*Δ+*RTS1* (OKA)	0.73	
4E	WT+vector (30˚)	1	
4E	WT+*RTS1* (30˚)	0.81	
4E	*gcn5*Δ+vector (30˚)	0.19	*2.2×10^{-4}
4E	*gcn5*Δ+*RTS1* (30˚)	0.28	**5.1×10^{-2}
4E	WT+vector (37˚)	1	
4E	WT+*RTS1* (37˚)	1.22	
4E	*gcn5*Δ+vector (37˚)	0.236	*3.4×10^{-3}
4E	*gcn5*Δ+*RTS1* (37˚)	0.36	**1.9×10^{-4}
5A	WT+vector (*HTA1*)	1	

5A	WT+*RTS1* (*HTA1*)	1.06	
5A	*gcn5*Δ+vector (*HTA1*)	1.05	
5A	*gcn5*Δ+*RTS1* (*HTA1*)	1.07	
5A	WT+vector (*HTB1*)	1	
5A	WT+*RTS1* (*HTB1*)	0.43	*$8.5x10^{-4}$
5A	*gcn5*Δ+vector (*HTB1*)	0.24	*$9.3x10^{-4}$
5A	*gcn5*Δ+*RTS1* (*HTB1*)	0.72	**$2.1x10^{-2}$
5A	WT+vector (*HTA2*)	1	
5A	WT+*RTS1* (*HTA2*)	1.14	
5A	*gcn5*Δ+vector (*HTA2*)	0.40	*$3.4x10^{-3}$
5A	*gcn5*Δ+*RTS1* (*HTA2*)	0.68	**$1x10^{-2}$
5A	WT+vector (*HTB2*)	1	
5A	WT+*RTS1* (*HTB2*)	1.13	
5A	*gcn5*Δ+vector (*HTB2*)	0.28	*$1.2x10^{-3}$
5A	*gcn5*Δ+*RTS1* (*HTB2*)	1.01	**$1.4x10^{-3}$
5A	WT+vector (*HHT1*)	1	
5A	WT+*RTS1* (*HHT1*)	0.44	*$4x10^{-3}$
5A	*gcn5*Δ+vector (*HHT1*)	0.48	*$3.4x10^{-5}$
5A	*gcn5*Δ+*RTS1* (*HHT1*)	0.83	**$9.3x10^{-4}$

5A	WT+vector (*HHF1*)	1	
5A	WT+*RTS1* (*HHF1*)	0.78	
5A	*gcn5*Δ+vector (*HHF1*)	0.42	*$7.1x10^{-3}$
5A	*gcn5*Δ+*RTS1* (*HHF2*)	0.76	**$2.7x10^{-2}$
5A	WT+vector (*HHT2*)	1	
5A	WT+*RTS1* (*HHT2*)	1.36	
5A	*gcn5*Δ+vector (*HHT2*)	0.63	*$3.6x10^{-2}$
5A	*gcn5*Δ+*RTS1* (*HHT2*)	0.82	**$1.5x10^{-2}$
5A	WT+vector (*HHF2*)	1	
5A	WT+*RTS1* (*HHF2*)	1.04	
5A	*gcn5*Δ+vector (*HHF2*)	0.83	*$4.2x10^{-2}$
5A	*gcn5*Δ+*RTS1* (*HHF2*)	1.06	**$2.4x10^{-2}$